DESIGN AND DEVELOPMENT OF SOFT & FLEXIBLE RE-PROGRAMMABLE MAGNETS

by

Can Berkay Akkaya

B.S., Mechanical Engineering, Middle East Technical University, 2022

Submitted to the Institute for Graduate Studies in
Science and Engineering in partial fulfillment of
the requirements for the degree of
Master of Science

Graduate Program in Mechanical Engineering
Boğaziçi University
2024

ACKNOWLEDGEMENTS

I would like to thank to my supervisor Evren Samur, who supported me in every subject as much as he could, and to Günay Züngör, Volga Yavuz, Berkhan Bayraktar, Uğur Dinçer for their support throughout my thesis and Şafak Güney for his friendship. I would also like to thank my family who made this thesis possible.

This project was supported by the Boğaziçi University Research Fund grant number 19782, and the Boğaziçi University Robotics and AI Laboratories Project (ROYAL) funded by the Presidency of Strategy and Budget of the Republic of Türkiye. We thank Assoc. Prof. Mustafa Öztürk from the Department of Physics at Gebze Technical University, and Uğur Topal from the Magnetism Laboratory at TÜBİTAK-UME for the VSM analysis. We thank Boğaziçi Center for Targeted Therapy Technologies, CT3 for the SEM.

ABSTRACT

DESIGN AND DEVELOPMENT OF SOFT & FLEXIBLE RE-PROGRAMMABLE MAGNETS

This thesis explores the development of a small-scale soft magnetic device. It introduces a novel reprogrammable magnet called soft and reprogrammable permanent magnet (srPM). The device is capable of remote magnetization with applied external magnetic fields. The working principle is similar to an electro-permanent magnet. A literature review including reprogramming strategies and electro-permanent magnets is presented. The objectives of this research are to design, fabricate and evaluate srPMs capable of remote magnetization. The srPM allows for magnetization via external magnetic pulses which is novel in the field of magnetic soft robots. Magnetic and mechanical experiments are implemented for characterization such as Vibrating Sample Magnetometer, Scanning Electron Microscope analysis and tensile test. The experiment setups are designed and fabricated including electromagnets and a pulse magnetizer. The proposed srPM has potential applications in biomedical applications. Possible implication areas could be drug delivery, surgical procedures, diagnostics.

ÖZET

YUMUŞAK VE ESNEK YENİDEN PROGRAMLANABİLİR MIKNATISLARIN TASARIMI VE GELİŞTİRİLMESİ

Bu tez, küçük ölçekli bir yumuşak manyetik cihazın geliştirilmesini araştırmaktadır. Yumuşak ve yeniden programlanabilir kalıcı mıknatıs (srPM) adı verilen yeni bir yeniden programlanabilir mıknatıs tanıtılmaktadır. Cihaz, uygulanan harici manyetik alanlarla uzaktan mıknatıslanma yeteneğine sahiptir. Çalışma prensibi bir elektro-kalıcı mıknatısa benzer. Yeniden programlama stratejileri ve elektro-kalıcı mıknatısları içeren bir literatür taraması sunulmuştur. Bu araştırmanın amacı, uzaktan mıknatıslama yapabilen srPM'leri tasarlamak, imal etmek ve değerlendirmektir. srPM, manyetik yumuşak robotlar alanında yeni olan harici manyetik darbeler yoluyla mıknatıslanmaya izin verir. Manyetik ve mekanik deneyler, Titreşimli Numune Manyetometresi, Taramalı Elektron Mikroskobu analizi ve çekme testi gibi karakterizasyon için uygulanmaktadır. Deney düzenekleri elektromıknatıslar ve bir darbe mıknatıslayıcı dahil olmak üzere tasarlanmış ve üretilmiştir. Önerilen srPM biyomedikal uygulamalarda potansiyel uygulamalara sahiptir. Olası uygulama alanları ilaç dağıtımı, cerrahi prosedürler ve teşhis olabilir.

TABLE OF CONTENTS

LIST OF FIGURES

LIST OF TABLES

LIST OF SYMBOLS

A	Ampere
$\mathbf{B}$	Magnetic Field Intensity
BH_{max}	Maximum Energy Product
$\mathbf{H}$	Magnetic Field
H_c	Coercivity
H_{ci}	Intrinsic Coercivity
kA/m	Kilo Ampere/meter
kPa	Kilo Pascals
$\mathbf{M}$	Magnetization
MPa	Mega Pascals
M_r	Remanent Magnetization
M_s	Saturation Magnetization
mT	MilliTesla
N	Newton
T	Tesla
Vol	Volume
Wt	Weight
X_m	Magnetic Susceptibility
μ_0	Permeability of Free Space

LIST OF ACRONYMS/ABBREVIATIONS

2D	Two Dimensional
3D	Three Dimensional
AC	Alternating Current
AlNiCo	Aluminium-Nickel-Cobalt
CIPs	Carbonyl Iron Particles
DC	Direct Current
MNPs	Magnetic Nanoparticles
MR	Magnetorheological
MREs	Magnetorheological Elastomers
NdFeB	Neodymium-Iron-Boron
PDMS	Polydimethylsiloxane
PVC	Particle Volume Concentration
SEM	Scanning Electron Microscopy
SmCo	Samarium-Cobalt
VSM	Vibrating Sample Magnetometer

1. INTRODUCTION

1.1. Background

1.1.1. Soft Robotics

A soft robot can be defined as a system composed of compliant materials with autonomous behaviour [1]. A robot is categorized as a soft robot depending on the compliance of the material. The materials used have moduli in range of 10^4 to 10^9 Pascals, in the range of soft biological materials [1]. The use of soft materials over rigid counterparts, specifically in human-robot interaction scenarios, offers advantages providing safer contact and are better suited for handling sensitive objects.

A soft robot comprises all subsystems of traditional rigid robots, such as sensors, controller, computation system, power source, actuation system. The combination of sensing, power, communication, processing with the soft material delivers smart materials. They can be actuated by numerous stimuli responsive materials including magnetic [2–5], thermal [6, 7], electric [8], light [9, 10], fluid [11], chemical stimuli [12]. The use of responsive materials allowed actively reconfigurable structures [13, 14].

Among those stimuli responsive materials, magnetic materials can achieve various accurate and sophisticated deformations owing to their force and torque induced response to magnetic field [15,16]. External magnetic field is advantageous for realizing lightweight, untethered robots. It is relatively simple to accurately control magnitude, phase, direction and frequency of the magnetic field [17].

1.1.2. Hysteresis Curve

The magnetic characteristics of a material can be shown by a B-H or M-H curve. B is the magnetic field intensity, H is the applied magnetic field, M is the total magnetization. The relation between the B-H and M-H curve can be represented as

$$\mathbf{B} = \mu_0(\mathbf{H} + \mathbf{M}). \tag{1}$$

B-H curve represents the resulting magnetic flux intensity of a ferromagnetic material under the influence of magnetic field H. The hysteresis can be seen in Figure 1.1. The applied magnetic field causes the magnetic domains align. When the applied magnetic field is eliminated, the magnetic moments of the domains does not totally recover to their original orientation. That is called remanent magnetization M_r. The material acts as a permanent magnet. Large hysteresis loop implies maximum energy product, which indicates the energy loss to magnetize the material. Hard magnetic materials are associated with large hysteresis while soft magnetic materials are characterized by a narrow hysteresis. The remanance is the magnetization that remains after the material is magnetized and applied field is removed. The coercivity denotes the required opposite magnetization to ensure demagnetization i.e. the remanent magnetization is zero. As the applied magnetic field **H** increases, the magnetic moments are substantially aligned with the field, inducing a magnetization in the material **M**.

1.1.3. Magnetic Materials

How much a material becomes magnetized under external magnetic field can be denoted by magnetic susceptibility [18]. According to magnetic susceptibility(X_m), magnetic materials can be categorized into ferromagnetic ($X_m >> 0$), paramagnetic ($X_m > 0$) and diamagnetic materials ($X_m < 0$) [18]. Ferromagnetic materials can be classified into hard magnetic, soft magnetic and super-paramagnetic. Ferromagnetic materials can be strongly affected by the magnetic field [18, 19]. However, paramagnetic and diamagnetic generate weak forces and repulsion respectively with a near zero remanent magnetization [18, 20].

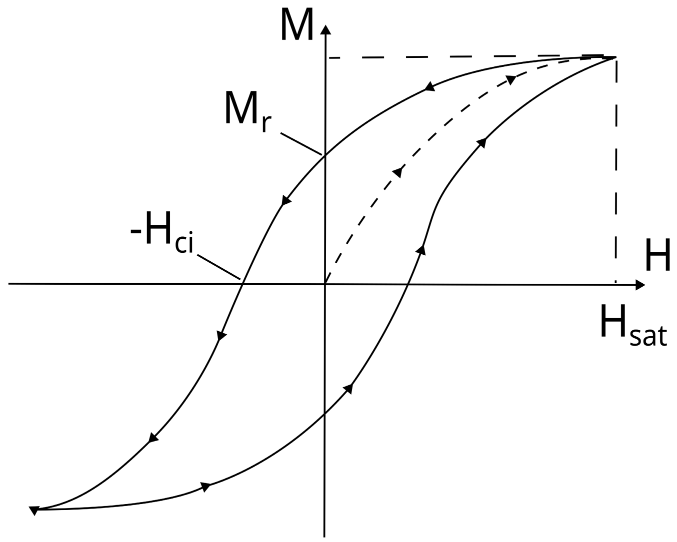

Figure 1.1. MH hysteresis curve. Arrows indicate the plot after initial magnetization. Intrinsic coercivity (H_{ci}), remanent magnetization (M_r) are shown.

There are three types of magnetic materials describing their ferromagnetic behaviour: soft magnetic, hard magnetic and super-paramagnetic. The hysteresis curves of ferromagnetic materials can be seen in Figure 1.2. Soft magnetic materials have high magnetic susceptibility and saturation magnetization. They have low remanence and coercivity making them easily magnetized and demagnetized by weak magnetic fields. They commonly refer to iron and iron-based alloys [21]. Hard-magnetic materials have high remanence and high coercivity. They can retain their magnetization when opposed by external magnetic fields. Common examples include chromium oxide (CrO_2), samarium-cobalt ($SmCo$) and neodymium-iron-boron ($Nd_2Fe_{14}B$) [21]. Superparamagnetic materials fall between the characteristics of soft and hard magnets. Their magnetization behaviour depends on particle size and shape, resulting in a near absence of remanence and coercivity [21]. Its noteworthy to emphasize semi-hard magnets are appealing such as AlNiCo which falls in between hard and soft magnet, having relatively low coercivity and high remanance.

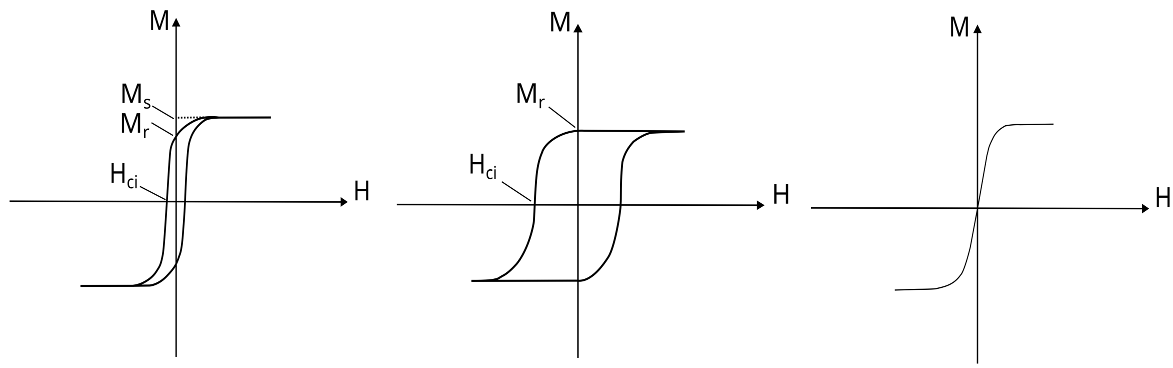

Figure 1.2. MH curves of (a) soft magnetic, (b) hard magnetic, (c) super-paramagnetic materials.

1.1.4. Electropermanent Magnets

An electro-permanent magnet (EPM) is a type of magnet that can be switched on and off using an electrical source. It maintains its magnetic state as if it were a permanent magnet [22]. Energy is only consumed during the switching process of the EPM. EPM consist of two magnetic parts: a hard magnetic material (NdFeB) and a semi-hard magnetic material (AlNiCo). Both magnets are enclosed in a coil [22, 23]. These hard and semi-hard magnets are arranged in parallel configurations so that their magnetization direction are either opposing or aligned in a single direction. It is activated through electrical means. The generated magnetic field by the coils magnetizes the AlNiCo either amplifiying or diminishing the magnetic field produced by NdFeB. When the magnetization directions of AlNiCo and NdFeB are opposite, the magnetic flux circulates within the system, resulting in a nearly negligible magnetic field. Conversely, when their magnetization directions are aligned, the system behaves as a permanent magnet. An electromagnet configuration was developed in millimeter scale by Knaian in 2010 [22]. An EPM design can be seen in Figure 1.3

The working principle of EPM makes it convenient and desirable when the magnetic field or magnetically inducible components of soft robots are wanted to be controlled. There are various applications that has been studied in the recent years.

Switchable electromagnets are used for MR fluid valves [24–26] and actuation [27–30], pneumatic valves [31],stiffness modulation [32], grasping [33]. Out of the scope of soft robotics it is used in industrial applications [34] and as a programmable matter [35].

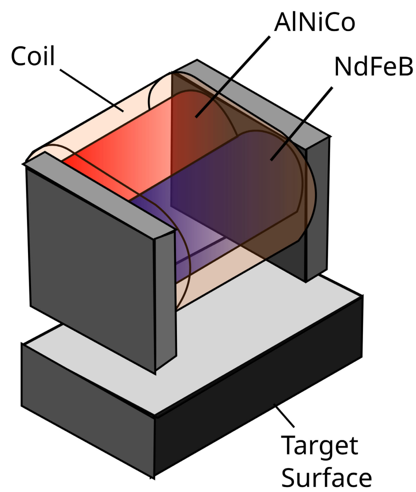

Figure 1.3. An electro-permanent magnet.

1.1.5. Soft Materials

Soft magnets are already introduced previously. To prevent ambiguity magnetic materials should be clearly defined, discriminating a soft magnetic material with a soft material. The term, soft material, refers to the mechanical behaviour of the material, while soft magnetic material refers to its magnetic behaviour.

<u>1.1.5.1. Matrix Materials.</u> The elasticity of the magnetic soft materials is given by polymeric composites [21]. The interaction of the magnetic filler particles to an actuating magnetic field shapes into an overall behaviour of the composite. The induced internal mechanical stresses is led by a deformation of the composite.

Silicone based thermosetting elastomers are commonly used for polymers due to ease of handling during manufacturing processes. Such materials include Sylgard 184 (Dow Chemical) [36], Ecoflex 00-10/00-20/00-30 (Smooth-On, Inc), and Elastosil

RT604/RT625/RT745 [37] or M4601/M4644 (Wacker Chemie AG) [38]. They are composed of commonly two separate parts and start curing when the parts are mixed or catalyst is added. The mixture can be easily poured into molds and cured. Thermoplastic elastomers can also be used. Those include styrene-ethylene-butylene-styrene (SEBS) [39]. At elevated temperatures, physical cross-links disentangle and filler particles can be mixed into the elastomer.

Gels are semisolids embodied with networks of colloidal or cross-linked polymers containing trapped liquids [40]. Gels are much softer than polymers. In context of soft robots the focus is mainly on cross-linked gels. When the swelling agent is water, they are referred to as hydrogels. When the swelling agent is oils or organic solvents, they are referred to as hydrogels [21]. Organogels include styrene-ethylene-butylene-styrene (SEBS) or styrene-butadiene-styrene (SBS) swollen in parafin or mineral oils [41].

1.2. Motivation

The re-programmability of magnetic soft robots has expanded capabilities in terms of maneuverability and adaptability. Some research studies have showcased their potential in various biomedical applications, including targeted drug delivery [42, 43], minimally invasive surgery [42,44,45], and biopsy [3,46]. This study introduces a novel magnetic material that can be reprogrammed remotely using only an external magnetic field. The srPM can change state with a short duration, low energy external magnetic pulse. This novel concept of *in-situ* magnetic reprogramming and reconfiguration of small-scale soft robots goes beyond the current state of the art. This approach enables the wireless manipulation of small-scale soft reprogrammable robots. srPM offers a novel method for altering the magnetization domain through magnetic pulses. It addresses a gap in the existing literature. This novel in-situ re-programmability feature will enable the robot to change its configuration during operation, and enhance the robots adaptability to different tasks during operations. For the future, a soft robot with task accomplishing capability can be constructed from few of these small-scale reprogrammable magnet devices securely bonded together. These magnets can be actuated to undergo shape changing through a reprogrammable magnetization profile while the profile can be adaptively controlled via remote magnetic source. Possible application areas are biomedical devices, drug delivery, meta-materials, origami, kirigami robots. Soft millimeter scale robots using srPM will enhance its operation capabilities. It can be used where magnetic actuation takes place. Softness and flexibility are required as compliance contributes to maneuvering. Angular structures use bends and flexibility to increase mobility. they also offer a safer structure for human interaction.

1.3. Objectives of the Study

Purpose of this study is to design a soft reprogrammable magnet, and evaluate its characteristics under different tests and compositions.

Objective 1: To develop and fabricate a soft, re-programmable permanent magnet capable of remote magnetization and demagnetization.

Objective 2: To build a test setup for performing magnetization and demagnetization of srPMs.

Objective 3: To demonstrate the on and off states and perform remote switching.

1.4. Literature Review

1.4.1. Magnetic Flexible Materials

The magnetic elastomers can be characterized by their magnetic components based on material properties. They can be made from hard magnetic or soft magnetic elastomers [47]. They can be referred to as magneetorehological elastomers (MRE), magnetoactive elastomers (MAE), magneto responsive elastomers [48].

MEs generally include elastomers with embedded hard or soft magnetic materials with a certain volume percentage and usually cured in a heat chamber to prevent settling out. The isotropic MEs are cured in the absence of a magnetic field. In anisotropic MEs it is shown greater response in terms of shear stresses and magnetic attraction forces [49]. For a n isotropic ME, it is possible to become an anisotropic ME when subjected to a suficient magnetic field, as the particles break and rotate in the elastomer [50]. Some researchers such as Dormann and Ogden, also studied to model and predict the magnetoelastic behaviour of isotropic MEs [51].

It is generally referred to as MREs when the material properties are concerned such as modulus, stiffness, damping capacity [52]. Magnetostriction namely shape changing behaviour is demonstrated at a maximum 10% for MRE [53].

1.4.2. Magnetic Soft Robots

In this section, some of the relevant studies in the field of magnetic soft robots, (re)programmable magnetic soft robots with shape-changing capabilities, clinical applications, and programming strategies are investigated.

Magnetic source is an appealing method offering wireless force generation and transmission, decoupling from the mechanical connections [54]. A magnetic source is capable of providing required power and control of the robot [55]. The magnetic source can be provided by an electromagnetic-coil system or moving permanent magnets [56].

Magnetic soft robots inherit magnetic materials with different concentration and configuration [57–59]. In an isotropic composite magnetic field induces dipole-dipole interactions between close particles when magnetized by an magnetic field. Magnetized particles tend to align with the applied magnetic field. The physical change in the microscopic level leads to macroscopic response of the composite [60]. It is called magnetostriction effect [57, 59–63].

1.4.2.1. Force and Torque Generation. An anisotropic composite can be obtained by applying magnetic field during curing of fabrication of the composite. The magnetic particles create chain like structures and solidify. When a magnetic field is applied to this chain-like magnetic composite, force between the magnetic particles help them preserve interparticle orientation while opposing mechanical deformation [64, 65]. Therefore the stiffness is increased. It is called magnetorheological effect.

To produce magnetic torques, a magnetic anisotropy is needed. Magnetic anisotropy is achieved by forming chains of isotropic particles [66–68] or using anisotropic filler particles (i.e. non spherical shapes) [69–71]. The response of soft magnetic materials can be seen in Figure 1.4.

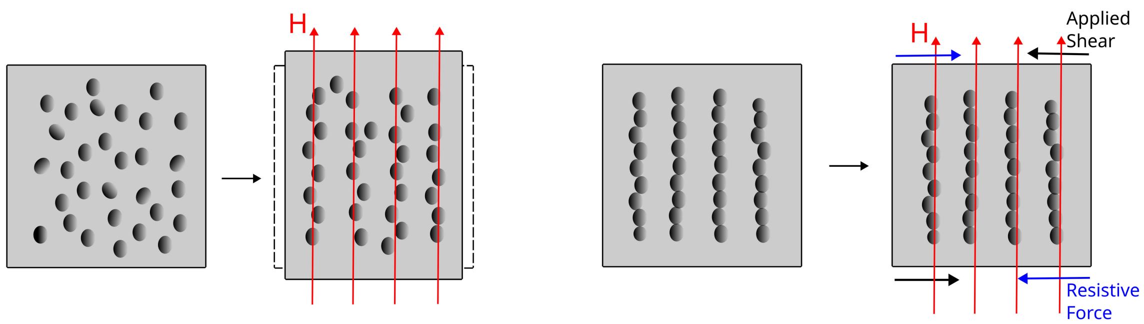

Figure 1.4. The response of soft magnetic materials. (a) Magnetostriction of isotropic soft magnetic composite. Particles are randomly dispersed. (b) Field induced stiffening of soft magnetic composite.

For hard-magnetic materials magnetic torques can be deployed since they have a remanent magnetization. The magnetic torque increases with the applied magnetic field below the coercivity. When a magnetic field applied the embedded particles head to align themselves with the actuating field [5]. For such bending applications both isotropic and anisotropic particles can be used.

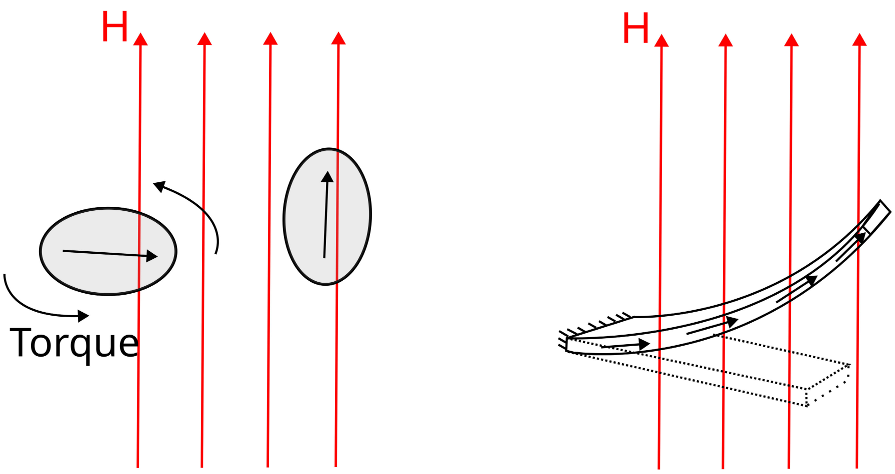

Figure 1.5. Torque driven bending of hard magnetic materials. (a) Magnetic torque acting on a single magnetized hard magnet. (b) Hard magnetic rectangular shaped composite that is uniformly magnetized, under uniform magnetic field. The magnetic field is perpendicular to the beam's remanent magnetization. Black arrows indicate remanent magnetization.

For magnetic composites embedded with soft magnetic particles when a magnetic field is applied the particle-particle interactions deform the matrix leading to an overall deformation, which is called magnetostriction. The introduced strain also allows to control the stiffness change. When a gradient magnetic field is applied the magnetic force per volume induced by the soft magnetic particles are expressed as

$$\mathbf{F} = \nabla \mathbf{B} \cdot \mathbf{M}, \tag{2}$$

where $\nabla\mathbf{B}$ represents gradient of magnetic field intensity. When a magnetic field is applied on to a composite embedded with hard magnetic particles, if the magnetization direction is not aligned with the magnetization of the particle, a magnetic torque is generated to align the direction. The induced torque per volume is expressed as

$$\tau = \mathbf{M} \times \ \mathbf{B}. \tag{3}$$

1.4.2.2. Remarkable Researches. In this section it is given some of the substantial developments in magnetic soft robots.

In 2018, Hu et al. produced a rectangular-sheet-shaped magneto-elastic soft robot [5, 72]. The composite is made of silicone elastomer namely (Ecoflex 00-10) embedded with hard magnetic neodymium-iron-boron particles. It is produced by wrapping it around a cylindrical object and cured under a present magnetic field. The robot is programmed to have a single-wavelength magnetization profile and is controlled by a time-varying magnetic field. It can swim inside and on the surface of liquids, climb liquid menisci, roll, and walk on solid surfaces, jump over obstacles, and crawl within narrow tunnels. It can additionally execute pick-and-place and cargo-release tasks.

Kim et al. presents a submilimeter scale self lubricating continuum robot with magnetic steering abilities [73]. It is fabricated by 3D printing and injection molding with NdFeB embedded inside the PDMS. It can reach targeted aneurysms and provide a lase beam when incorporated by optical fibers.

1.4.3. Magnetic Programming

Similar to this study, based on physical alignment and fixing of the magnetic particles inside the composite during curing, magnetic programming approaches are introduced for encoding discrete 3D magnetization profiles in small-scale soft materials [74–76]. It is used lithographic or 3D printing techniques, the magnetization profile of the material is adjusted according to a certain task.

The programming magnetization profile (encoding magnetic anisotropy) has two common techniques where making magnetization after fabrication and magnetization during fabrication. In the first method magnetic particles are fixed during the fabrication. The manufactured part is then magnetized under strong magnetic field ($> 1T$) in undeformed or folded, bended position [15, 72, 77]. Due to single mode of deformation they are suitable for applications like locomotion,soft grippers. The magnetic anisotropy allows for limited shape-modes. In the other method, the magnetization profile can be programmed during manufacturing such as photolithography [74] or 3D printing [75]. The principle is that when the polymer is locally cured, a magnetization pattern can be formed selectively. However, once the magnetization anisotropy is fixed it can not be changed. This method allows more complex shape changing modes.

Spacial programmability is achieved by jig-assisted assembly [15], lithography [74,78], 3D printing [75], local heating of magnetization profiles [79], direct laser writing [80].

1.4.4. Magnetic Re-programming

Reprogramming refers to the ability to modify the magnetic properties of a material to suit specific needs or applications. This typically involves changing the direction, strength, or configuration of the material's magnetization [81,82]. Re-programmability is a very important feature in magnetic soft robotics because it allows the robot to adapt to different tasks, environments or requirements without the need for physical changes or modifications [81, 82]. For reprogrammable magnetic soft actuators, hard magnetic composites (i.e. NdFeB, SmCo) are preferably used as materials [46,79,83–85]. Various approaches have been proposed for reprogramming magnetization techniques.

In 2020 Alapan et. al proposed a reprogramming strategy of hard-magnetic particles which is heating the material above the Curie temperature of the ferromagnetic particles and then reorienting the magnetic domains with the application of an external magnetic field during the cooling process for magnetic shape-morphing [79]. On reaching a magnetic material's Curie temperature, the spontaneous magnetization in the material drops to zero. At this point, the material is no longer a ferromagnetic material, instead becoming a paramagnetic material. A material's magnetic moment (which is a dipole moment within in atom originating from the spin and angular momentum of electrons) determines the force of magnetism. Different materials have unique structures of intrinsic magnetic moments and the alignment of these intrinsic magnetic moments is dependent on temperature.

To reprogram magnetic materials, phase-change materials with relatively low melting temperatures, such as polyethylene glycol [46] or polycaprolactone [83], are also used to encapsulate the magnetic particles in the polymeric matrix.

In 2022, G. Dong *et al.* developed a magnetic vitrimer with magnetic particles mixed with a polymer network containing abundant dynamic covalent bonds [86]. When the temperature is elevated to the exchange temperature of covalent bonds, the viscous magnetically responsive material goes under large deformations, . Magnetic vitrimer (MV) is produced of epoxy monomers (EPS 25) stoichiometric mixtures of two sulfhydryls (EDDET and PETMP) that are embedded with magnetic particles (Fe3O4) into the polymer matrix. The monomers consist of abundant disulfide bonds and the bond exchange reaction becomes more active at elevated temperatures resulting in increased flowability of the composite.

In 2023, W. Li *et al.* proposes a self-vectoring electromagnetic soft robot (SESR) demonstrating shape morphing and locomotion capabilities that are unachieved before [87]. Here, a distinction is made between external and internal magnetic actuation for vector control, where the aforementioned magnetic actuation is performed by only external magnetic field vectors. The proposed concept of self-vectoring control adjusts the interior vectors of every sub-domain of the robot, realizing actuation under passive and constant fields. It is designed with two magnetic coils, a planar spiral and a 3D helix which corresponds to vertical flux actuator (module V) and horizontal flux actuator (module H), respectively.

In 2024, there has been studies which uses the heat requirement to allow re-rotate the magnetic particles inside the liquefied polymer [88]. Under magnetic field magnetic particles realigns with the field and the polymer is solidified. Apart from this, Johnson and Kramer-Bottiglio proposed a compliant EPM that mixes AlNiCo and NdFeB magnetic powders in a matrix [89]. Although they have achieved a soft

EPM that can carry its own weight and vice versa in the OFF state, the magnetization in OFF states is not close to zero because mixing magnetic particles leads to magnetic interaction of the adjacent powders [90, 91]. Besides, the magnetic flux density is not close to zero on the surface at the OFF state due to the lack of the directed alignment of the magnetic field that is normally achieved by magnetic caps of EPMs. Therefore, there is still a gap in the field in terms of efficiently and remotely reprogrammable magnetic soft robots.

In 2025, Sodomka and Mach made electro-permanent elastomer (EPE) that can be switched on and of similarly to an electro-permanent magnet [92]. Two ferromagnetic materials namely, NdFeB and strontium ferrite (SF-D360) are mixed with Dragon Skin FX-PRO. The size of the samples are 17x17x2.5 mm. They achieved 67 mT of remanent magnetization in the ON and 2.1 mT remanent magnetization in the off state. Their EPE needs 620 mT to change between states, which is quite challenging to apply externally.

Sun *et al.* present dynamic reprogrammable magnetic soft machine (drMSM) including a flexible resonant circuit [93]. It is achieved addressable and perceptible heating of specific regions. It consist of multiple branches of an inductor, a capacitor, a resistance wire connected in series. By adjusting capacitance in each branch, distinct resonant frequencies are defined. A heating field selectively heat specific branches matching the resonant frequency. When the low-melting alloy starts to melt the NdFeB inside the liquid chamber starts to align with the applied magnetic field.

2. DESIGN OF THE SOFT REPROGRAMMABLE PERMANENT MAGNET

2.1. Working Principle

The working principle is similar to principle of an electro permanent magnet. The srPM states are formed by changing the magnetization direction of the inherent soft magnet. NdFeB magnet is selected due to its high remanance and high coercivity and AlNiCo magnet is selected due to its high remanance and low coercivity. This allows changing remanent magnetization of AlNiCo by an externally actuating field without affecting the remanent magnetization of the NdFeB. The direction of the soft magnet, AlNiCo, can be adjusted. When the direction of both AlNiCo and NdFeB are the same they set an apparent magnetic field in one direction. When the direction of both AlNiCo and NdFeB are the opposite their magnetic field dampen down each other. The working principle can be seen in Figure 2.1.

The concept of the srPM is based on a permanent magnet setup having two operation states depending on its magnetic flux density. In the ON state, the srPM acts like a permanent magnet, and in the OFF state, the magnetic flux density of the srPM is reduced to zero. The srPM consists of one hard magnet, NdFeB, and one semi-hard magnet, AlNiCo,

As in the case of a real electromagnet, MRE caps are ought to be router and concentrates the field passing inside, since the permeability of MRE is much higher than the air.

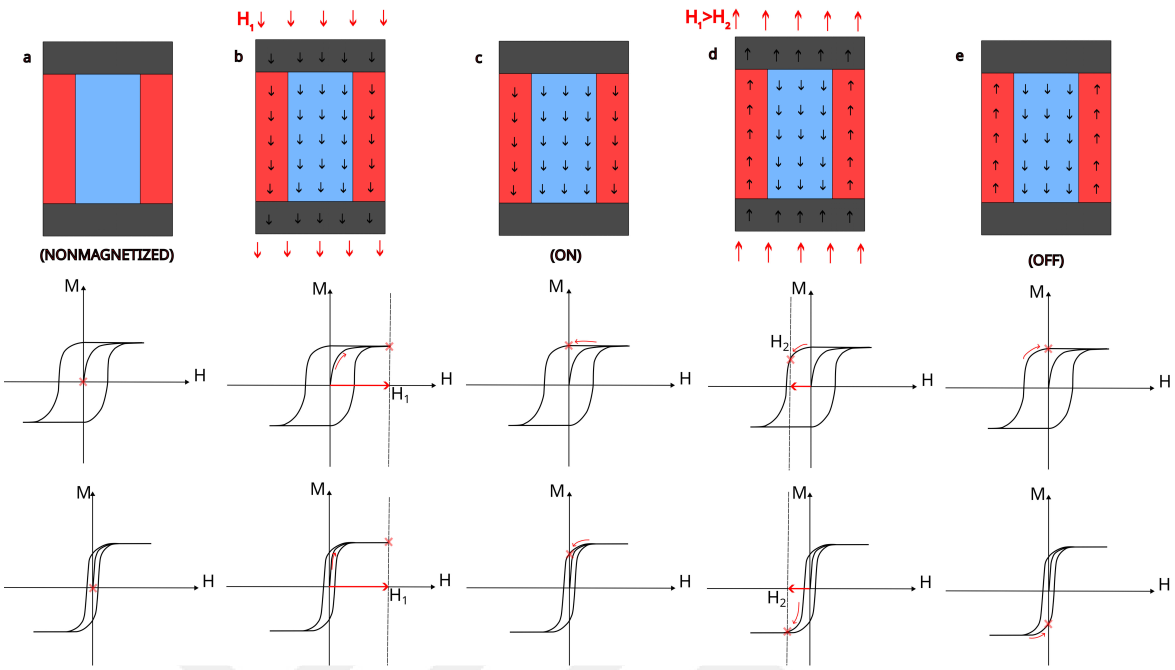

Figure 2.1. Working principle of the srPM. (a) Nonmagnetized. (b) It is magnetized by a saturating magnetic field $H_1 > H_{sat}$. (c) The magnetizing field is removed. The remanent magnetization of both magnets are in the same direction. The srPM is in ON state. (d) A magnetic field $H_c < H_2 < H_1$ is applied. AlNiCo is magnetized in the reverse direction. (d) The magnetic field is removed. The srPM is in OFF state.

2.2. Design Iterations

Determining the geometry and the volume fractions of the composite are design parameter that have been worked on. Initial conceptual design is formed on the bases of the geometrical similarity of an actual electro-permanent magnet where two different magnets aligns next to each other, creating a loop through ferrite poles. The initial conceptual design can be seen in Figure 2.2. AlNiCo and NdFeB composites are placed next to each other and MRE composites are attached to pole ends.

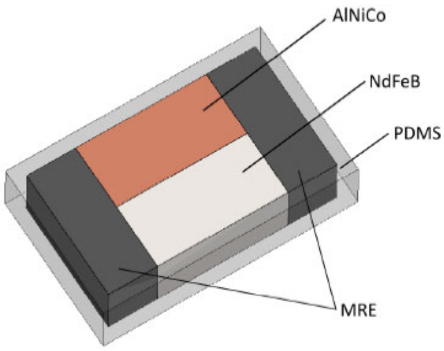

Figure 2.2. Initial conceptual design of soft and reprogrammable permanent magnet. AlNiCo and NdFeB rests next to each other, covered by a thin layer of PDMS.

The next iteration is in axis-symmetric configuration. The core AlNiCo cylinder is surrounded by a NdFeB hollow cylinder. MRE caps are attached at the pole ends. The design can be seen in 2.3

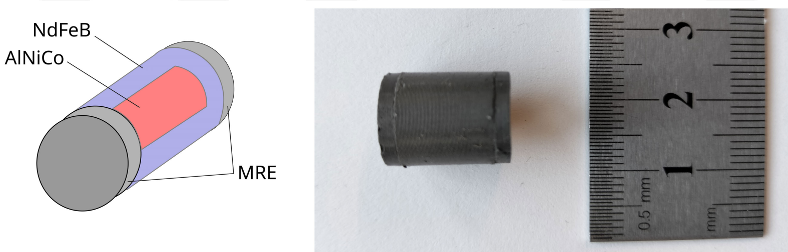

Figure 2.3. Iterated design. The geometry of the srPM is turned into axissymmetric configuration where AlNiCo positioned in the center and outer cylinder is made of NdFeB. The size of the srPM is 16 mm by 12 mm in diameter.

At this stage a prototype was fabricated. NdFeB matrix is composed of Ecoflex-0030 and nonmagnetized NdFeB powder. The volume fractions of the NdFeB powder, Ecoflex-0030 and PDMS oil are 40%, 40% and 20%, respectively. Similarly, semi-hard magnetic AlNiCo is blended with Ecoflex-0030. The volume ratio of the AlNiCo powder, Ecoflex-0030 and PDMS oil are 40%, 40% and 20%, respectively.

In the last iteration, the size of the srPM is downsized to 6 mm. The reason behind this downsizing is that the srPM should be as small as possible to increase application areas. The magnet composites is switched in the design for the ease of manufacturing. The NdFeB core is surrounded by AlNiCo. The design can be seen in Figure 2.4.

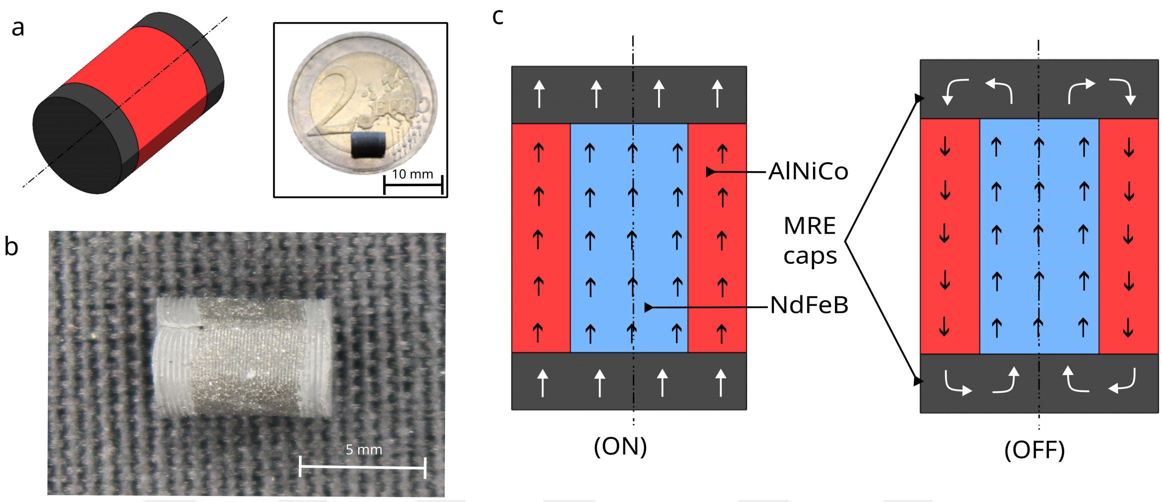

Figure 2.4. Soft and reprogrammable permanent magnet. (a) The prototype of the srPM is axially symmetric. It consists of a cylindrical NdFeB composite, a hollow AlNiCo composite, and two MRE caps at the ends. (b) A fabricated sample of the srPM, which has a length of 6 mm and a diameter of 4 mm, on a 2€. (c) In the ON state (left), the magnetization direction of the NdFeB and the AlNiCo are the same.

Further development on the basis of remanent magnetization and considering the maximization of the interaction between the NdFeB and AlNiCo, the design is iterated where both magnets are axis-symmetric and surrounds each other.

It is seen that when the design is optimized to have a near zero remanance in the OFF state, the radius ratio of NdFeB to AlNiCo becomes very small, resulting in an overall magnetic strength loss in the ON state. Thus is decided to have larger magnetic field strength values making the radius of both materials balanced. This results in more strength in the ON state and a residual magnetic field in the OFF state.

Various molding trials, 30%, 40%, 50%, 60% volume fractions of magnet powders are tried and it is observed that the solubility of the powder is maximum at 40%. To maximize the force in the ON state it is chosen 40% volume fraction for magnetic powders. The volume ratio of the AlNiCo is maximized to obtain the highest magnetic flux density.

2.3. Materials and Fabrication

SrPM is made of hard and semi-hard magnets. An srPM is composed of flexible NdFeB, flexible AlNiCo and MRE. Initially AlNiCo powder (American Elements) is mixed with Dragon Skin 30 (Smooth-On Inc.) with a volume ratio of 40% and degassed at a vacuum chamber. The mixture is poured in acrylonitrile styrene acrylate (ASA) molds that is shown in Figure 2.5 and iron bars are pressed in the centers of the mold. The mold is placed into an oven at 80° C and waited for 30 minutes. After the AlNiCo is cured, the bars are taken out and the core cylinder is filled with NdFeB mixture. NdFeB mixture is composed of Dragon Skin 30 and NdFeB powders (QP-S-11-9-20001, Magnequench, Co. Ltd.) with a volume ratio of 40% [94]. Pouring the uncured mixture on top of cured AlNiCo eliminates the need for adhesive. Cured flexible AlNiCo and NdFeB are replaced in another mold with a space at the end for MRE. The same procedure is repeated for MRE caps with carbonyl iron particles (CIP) (Nanokar). MRE parts are cured in two steps. In the first step one side is poured and cured. In the second step the other side is poured and and cured of an srPM. The fabrication process is illustrated in Figure 2.6. The molds can be seen in Figure 2.5.

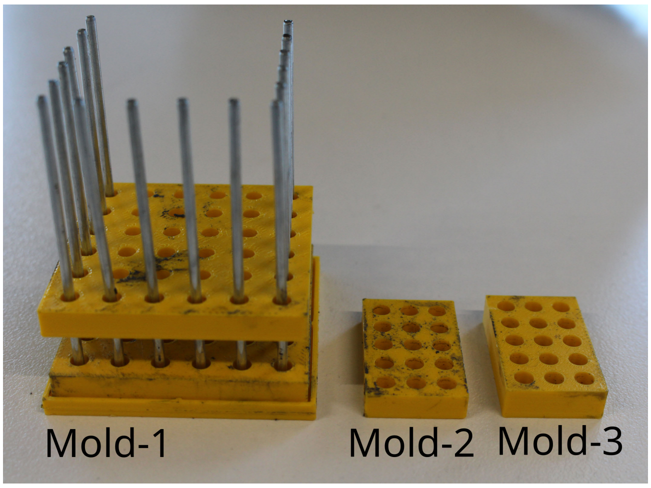

Figure 2.5. A photography of molds used in fabrication.

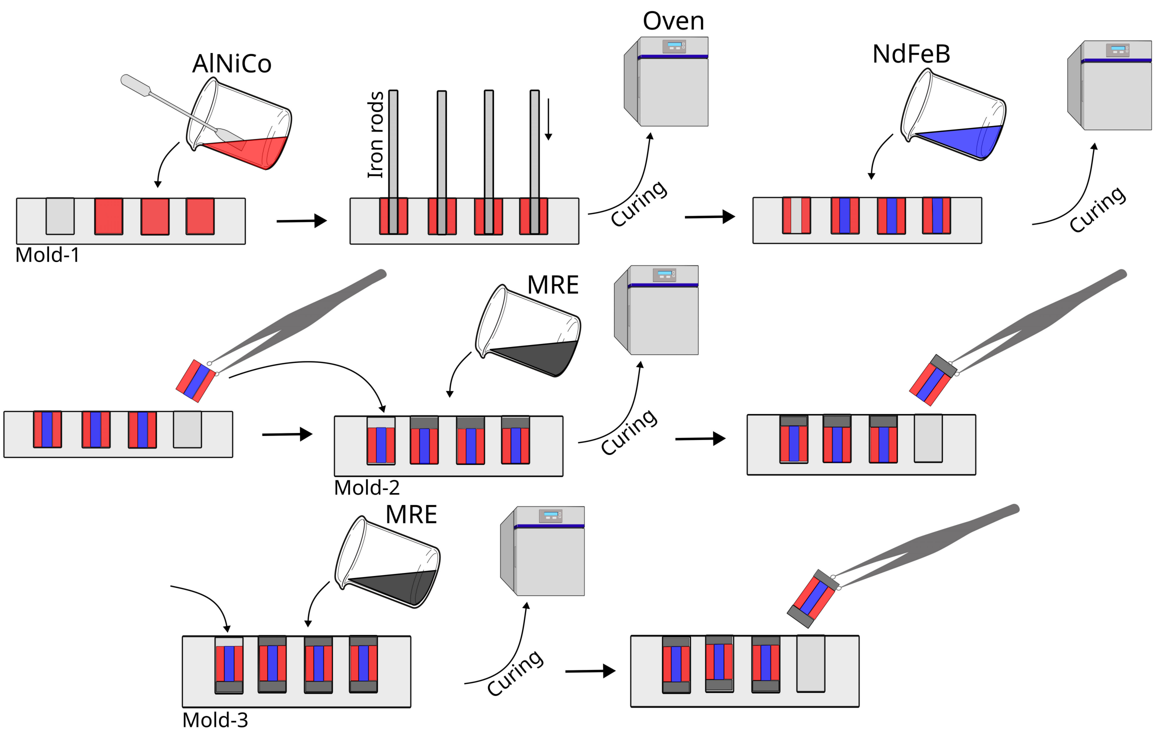

Figure 2.6. The fabrication of finalized version of srPM. Three molds used progressively. Firstly AlNiCo is poured and iron rods are pressed into center. After curing AlNiCo, NdFeB is poured where the rods are removed. After curing, the magnet is placed into the second and third mold to cure MRE caps.

2.4. Simulation

The simulation study is performed in Ansys Maxwell. The magnetic flux density of srPM in ON and OFF states are observed, the results are shown in Figure 2.7. The force exerted on an iron cap is measured.

The diameters of the flexible magnets are selected as design parameters, while the magnetic forces are used as the cost function. The magnetic force in the OFF state should be low enough that the magnet cannot support its own weight, whereas it is aimed to be maximized in the ON state. The geometry of the srPM is finalized in line with the result.

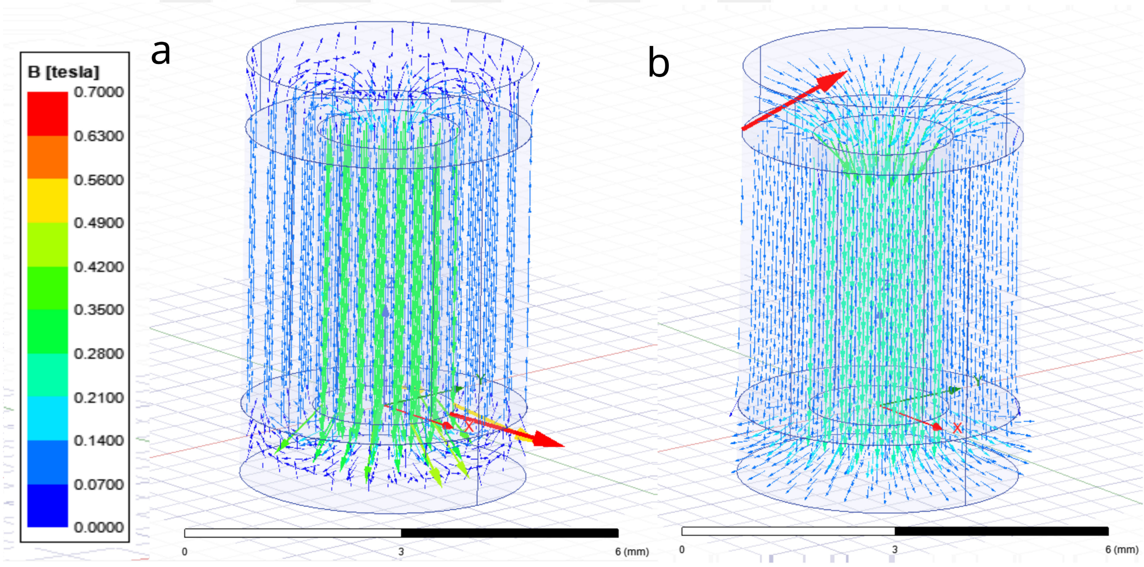

Figure 2.7. The simulation performed in Ansys Maxwell. The srPM in (a) OFF and (b) ON state.

The flexible AlNiCo and NdFeB components are modeled as simple permanent magnets, with their properties characterized using values obtained from VSM analyses. The MRE parts are modelled as soft magnets.

To validate the srPM model in the simulations, an iron piece is placed at the bottom of the srPM with a 0.1 mm air gap to measure how it is affected by the magnetic field generated by the srPM. The calculated attraction forces between the iron piece and the srPM module are 18 mN in the ON state and 5 mN in the OFF state, aligning closely with the experimental results.

2.5. Design of Electromagnet System

A twin electromagnet system is to be employed in a well-aligned configuration to serve as the external magnetic field generator. The critical task of determining the required external magnetic field strength for changing the srPM's state at a predetermined distance from external sources will necessitate analytical calculations and simulations. The design parameters include length of the coils, coil core materials, number of turns and current over the wires.

A soft magnetic material is preferred for the core due to its high magnetic susceptibility and permeability. In a DC application high permeability and low coercivity is desired. Some of the applicable soft materials commercially available are shown in Table 2.1.

Table 2.1. Properties of available core materials for electromagnets.

Material	**Composition**	μ_i	μ_{max}	**H (A/m)**
Iron	99 Fe	200	6000	7.2
50 Permalloy	50Ni-50Fe	-	100000	4
80 Permalloy	80Ni-20Fe	4000	100000	4
Supermalloy	79Ni-15Fe-5Mo-0.5Mn	90000	10^6	0.32

Considering material availability Permalloy-80 is chosen and obtained. Although iron is commertially available and easy to find the characteristics are not desired for this use. After selection of core material it is performed Comsol simulation to determine the geometry of the coils. It is required 50 kA/m of magnetic field to change the direction of the magnetization of AlNiCo. It is achieved 80 kA/m in the middle with a distance of 100 mm between the electromagnets. The simulation can be seen in Figure 2.8.

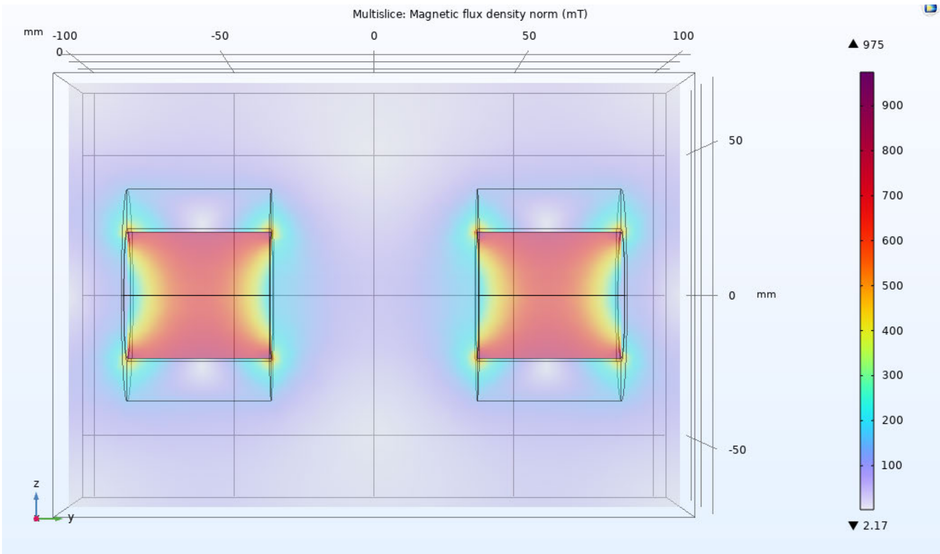

Figure 2.8. Simulation of electromagnet setup in Comsol. A parametric design is performed to obtain a necessary magnetic field in the center.

The circuit to drive the electromagnets are designed in Proteus. The initial requirement of the circuit is to supply required current with respect to calculated NxI from the simulation. The current should be reverseble to apply the magnetic field in opposite direction. From this demand it is thought a H-Bridge circuit including MosFets with high current and voltage ratings.

The driving voltage is selected as 48 V, applicable to supply from LED drivers. Since the driving voltage is relatively high it is required an optocoupler to connect the low voltage controller circuit to high voltage driving circuit. Mosfets are used to channel 48 V to electromagnets. The final manufactured electromagnet can be seen 2.9.

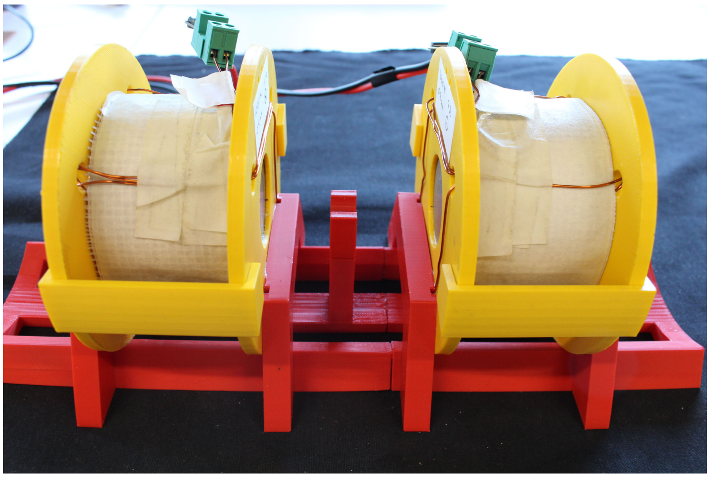

Figure 2.9. A photography of fabricated electromagnet setup.

2.6. Design of Pulse Magnetizer

In this section it is studied to design a magnetizer to magnetize an initially non-magnetized material. The main purpose is to mangetize the manufactured srPM samples. They consist of flexible NdFeB and AlNiCo magnets. Since the saturation magnetization of NdFeB is higher than AlNiCo the magnetizer should be able to magnetize NdFeB. It is required a 2 T of magnetic field to fully magnetize the NdFeB [94]. it is developed a magnetic pulse magnetizer using the principle of discharging the energy of the capacitors to energize coil windings [95].

The DC voltage is supplied by voltage multiplier to reach higher energy levels. The capacitors are charged in a DC circuit. The capacitor energy is expressed as **??**. After the energy in the capacitor is reached to a desired level, the charging circuit is detached. The capacitors are triggered by a thrystor circuit. When a trigger voltage exceeded, the thrystor gate allows the current flow in one direction. One of the keynotes is that it is required a direct current at the coil in one direction. And the reverse charging of the capacitor should be discharged in the same manner. It is utilized diodes to prevent reverse current over the coils. The pulse magnetizer circuit can be seen in 2.10. To achieve 2 T of magnetic field, a parametric design of the coil is simulated in Comsol, which can be seen in Figure 2.11. It is seen that NxI needs to be at least 70000. The winding is hold minimum to minimize the wire resistance. Number of turn is selected as 100. Thus, It is required a 700 A of pulse current in the coil. Afterwards, a circuit is designed considering a capacitor, inductor and a resistor in series. The circuit of the magnetizer can be reduced to an RLC circuit where the energy of the capacitors are channelled to coil. The fabricated magnetizer can be seen in Figure 2.12.

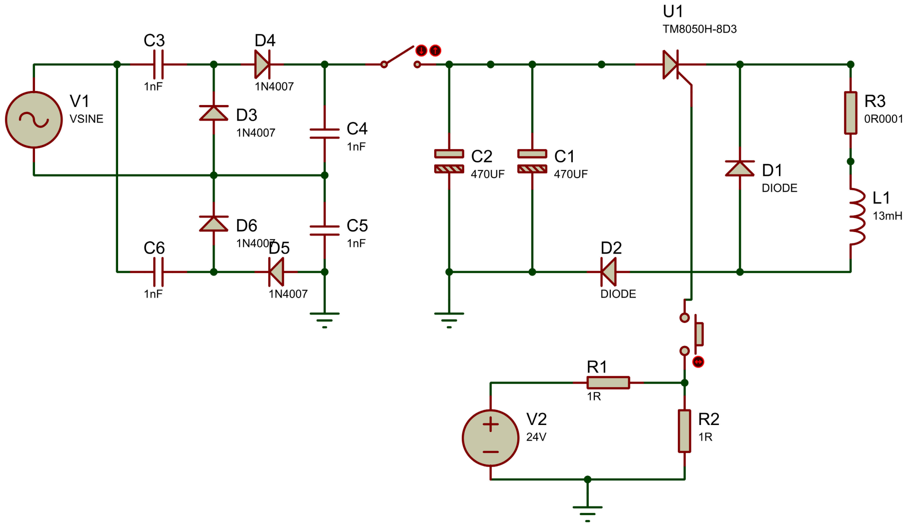

Figure 2.10. Designed circuit diagram of pulse magnetizer.

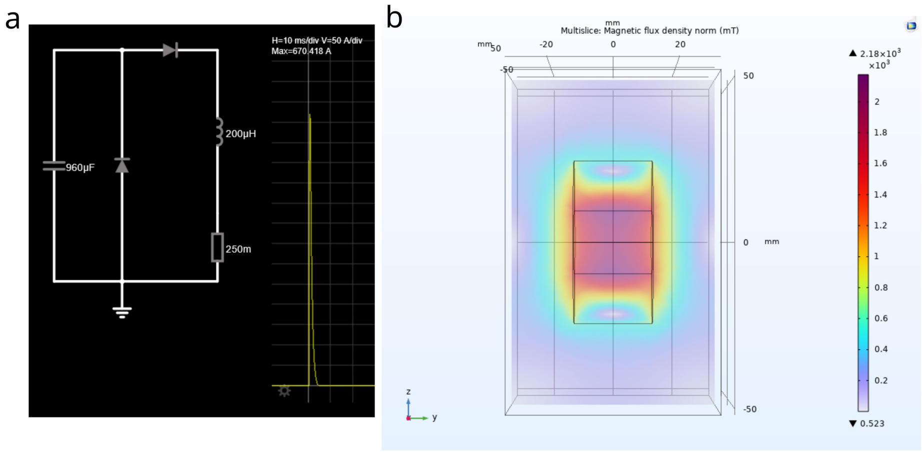

Figure 2.11. Simulation of pulse magnetizer (a) Circuit simulation in a redacted RLC circuit to obtain maximum current in the pulse. (b) Comsol simulation to verify the magnitude of the magnetic field in the center.

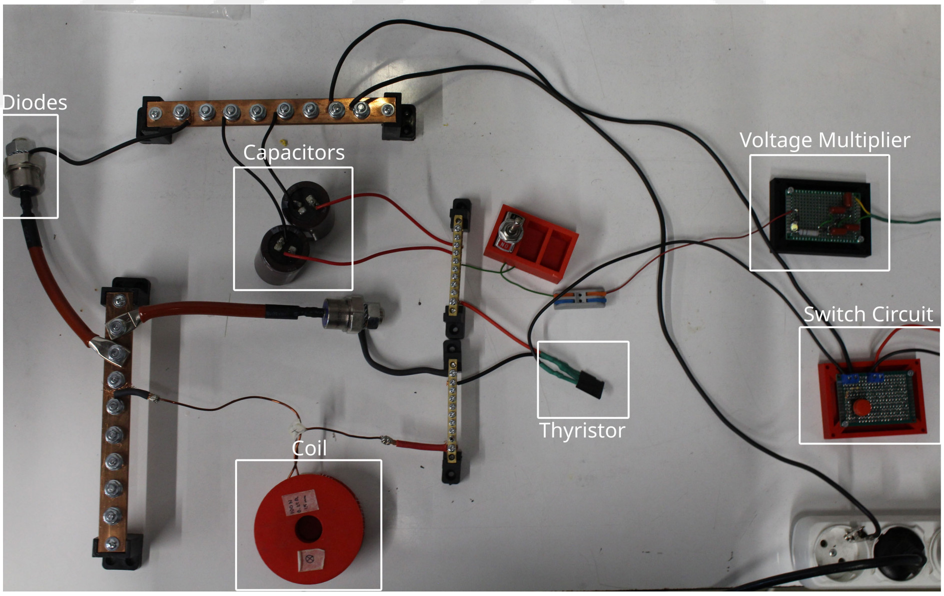

Figure 2.12. A photography of fabricated pulse magnetizer circuit.

3. EXPERIMENTS AND RESULTS

3.1. Magnetic Characterization

The magnetic measurements are taken from three srPM samples, for each ON and OFF states, on both sides, with five points per side. In the ON state, the magnetic field exerted by the module is 22.72 mT on average with a standard deviation of 0.35. In the OFF state, the magnetic field exerted by the module is 3.23 mT on average with a standard deviation of 0.26.

3.1.1. BH Curve of AlNiCo

3.1.1.1. Experimental Procedure. BH curve of a material is helpful for determining its remanance and coercivity. The BH curve of NdFeB is available from the manufacturers data [94], however it is not available for AlNiCo. The Vibrating Sample Magnetometer (VSM) (Quantum Design PPMS 9T) test is performed to obtain BH curve of the AlNiCo. The full magnetization curve is needed for the state change of the magnet as well as simulation purposes. Both powder and flexible AlNiCo is tested in the VSM.

3.1.1.2. Results. The obtained BH curves are shown in Figure 3.1. The coercivity of the AlNiCo-based flexible magnet is about 50 kA/m, and that of the NdFeB-based flexible magnet is about 250 kA/m. The remanence values of the magnets are 110 mT and 450 mT for the AlNiCo and the NdFeB, respectively.

3.1.2. Matrix Material Experiment

The matrix materials of the magnetic soft materials have great importance based on their mechanical properties and chemical stability. Since the prior studies suggest that the particles may rotate inside the elastomeric matrix [96], an experiment is designed to see how hard magnetic materials act on different matrix materials.

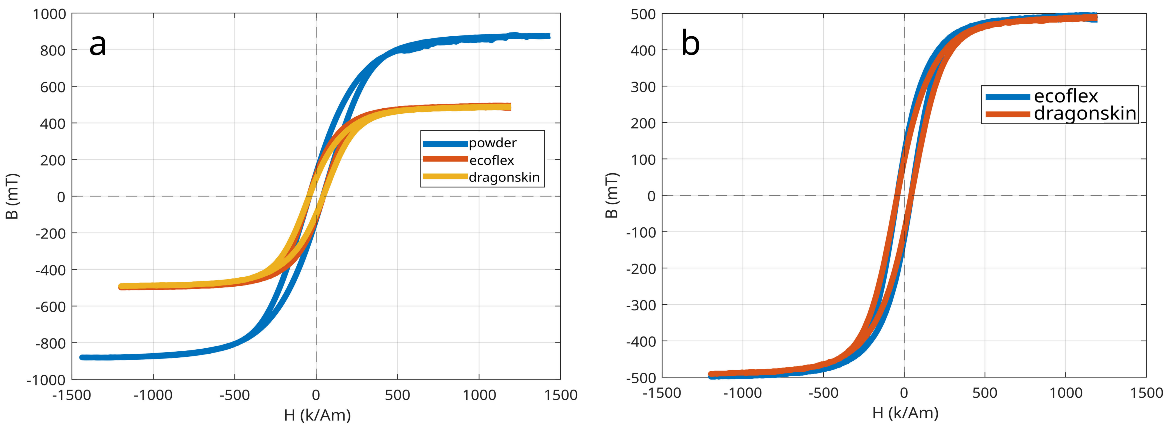

Figure 3.1. BH hysteresis curve of AlNiCo powder.

3.1.2.1. Experimental Procedure. Four matrix materials are tested to choose the appropriate one for this study. The first matrix material is Ecoflex 00-30 with low-viscosity (3000 cps) silicone oil. Silicone oil decreases viscosity at the uncured stage, facilitating the uniform mixing of magnetic powder into the elastomer and resulting in a softer, more flexible magnet after curing. The other matrix materials are Ecoflex 0030, Dragon Skin 30, and Sil 960. Cylindrical, flexible magnets with 10 mm diameter and 16 mm length were manufactured with different matrix configurations for AlNiCo and NdFeB. All flexible magnets include a 40% volume ratio of magnet powders. Matrix compositions are EcoFlex 0030 with a 20% weight ratio of silicone oil, EcoFlex 0030, Dragon Skin 30, and Sil 960, respectively. Prior to the test, all the samples are magnetized. Flexible magnets are exposed to pulses of varying magnitudes in the direction opposite to their magnetization, and their remanent magnetization is then measured. Magnitudes of the pulses are 0, 5, 10, 15, 20, 25, 30, 40, 60, 80, 100, 120, and 150 mT, respectively. The magnetic field applied in order from 0 to 150 mT, measurements taken each time. Three samples were tested from each matrix powder configuration, and six values were read from the flexible magnet's north and south surfaces from random points.

3.1.2.2. Results. The results given in Figure 3.2 indicate that as matrix materials get softer, the remanence magnetization of the flexible magnet decreases, and the flexible magnet becomes more susceptible to the applied magnetic field. The sample with silicone oil is affected most by the applied magnetic field. These results give clues about the reason for the sensitivity of the applied magnetic field. Adding silicone oil decreases the density of the cross-links in the polymer; this makes the polymer softer and easier to tear. Moreover, high viscosity of the Sil 960 prevents homogenous mixing of the elastomer with magnetic particles.

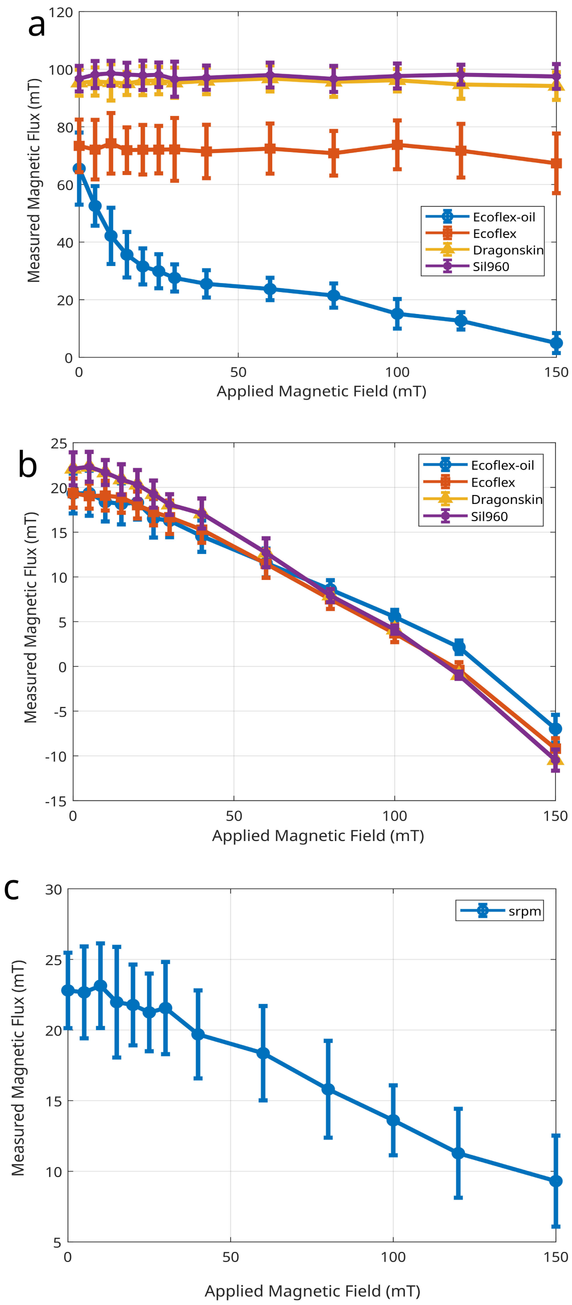

Figure 3.2. Results of the matrix material experiments for (a) flexible NdFeB magnets and (b) flexible AlNiCo magnets, (c) and the srPM. Each point is the mean of three specimens, and the error bar represents the standard deviation.

3.1.3. Force Measurement

The force applied by the srPM in ON and OFF states are measured. The srPM is attached to a 100 g load cell (DigiKey) on one end while the other end remains free. The srPM and load cell are free to move towards a fixed iron piece, the motion is controlled by a motor. The test is conducted with the same test setup with the mechanical characterization test with some modifications. The force measurements are taken at the point of contact. Data is collected for three repetitions for three srPM for both ON and OFF states. The modified version of the used setup can be seen in 3.4.

3.1.3.1. Experimental Procedure. The attraction force between the half-capsules is measured. The force is measured by gluing the tip of one of the half capsules to a fixed plate and the other to a moving plate connected to the 100 g capacity load cell. The test setup for the tensile test is rearranged by only changing the fixtures to hold the capsule. The force of attraction is recorded as each capsule half is moved away from the other with a speed of 0.2 mm/s.

3.1.3.2. Results. In the ON state, the srPM exerts a force of 19 mN, with a standard deviation of 0.38 mN. In the OFF state, the force decreases to 7 mN, with a standard deviation of 1.1 mN.

3.2. Mechanical Characterization

3.2.1. SEM Analysis

3.2.1.1. Experimental Procedure. Scanning electron microscope (SEM) images of three different matrix materials are collected to solidify the results obtained from the matrix material experiment. The SEM images of flexible NdFeB and AlNiCo magnets with matrix materials of Ecoflex 0030 with oil, Ecoflex 0030 without oil, and Dragon Skin

30 without oil with a magnification of 1000 times can be seen in Figure 3.3.

3.2.1.2. Results. SEM images reveal that there are cavities around the powders in the samples that contain silicone oil. AlNico particles in the sample containing silicone oil catch the elastomer matrix, despite the cavities, thanks to their uneven shapes; however, the NdFeB particles seem free to rotate inside the matrix due to their spherical shape. This observation supports the results of the matrix material experiments, which showed minimal changes in the behavior of AlNiCo magnets, whereas the NdFeB magnets exhibited more significant differences. Those results indicate that the change in the remanence magnetization after exposure to low magnetic fields is probably caused by the physical movements of the particles rather than the particles' internal magnetic domains. It is seen that there are cavities around the NdFeB powders in the samples with silicone oils. It is concluded that the change in the remanence magnetization of flexible NdFeB magnets is not caused by minor hysteresis curves but instead is caused by the mechanical rotation of the powders inside the matrix, supported by the results obtained from SEM.

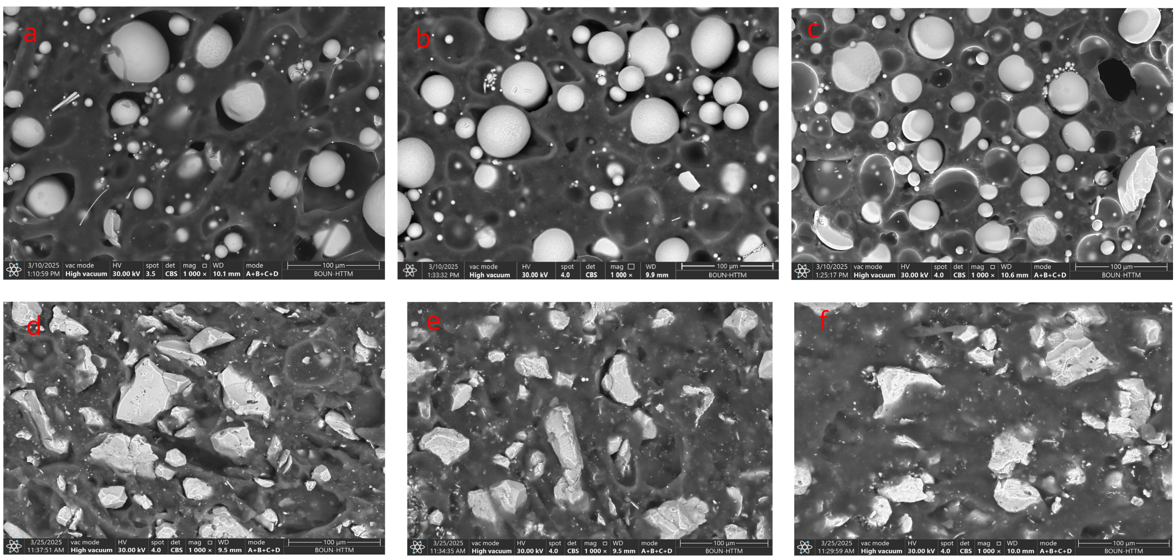

Figure 3.3. SEM images of (a) the EcoFlex 0030 with oil, (b) EcoFlex 0030 without oil, and (c) Dragon Skin 30 without oil. SEM images of AlNiCo samples are shown with (d) EcoFlex 0030 and oil, (e) EcoFlex 0030 without oil, and (f) Dragon Skin 30 without oil. The images are 1000 times magnified.

3.2.2. Tensile Tests

3.2.2.1. Experimental Procedure. Mechanical characterization is essential for the design of robots based on the srPM. These tests are performed using a custom-built tensile test platform designed for precision and control. The platform is built on linear rails and is controlled by a micrometer driven by a Nema 17 stepper motor controlled by an Arduino Uno. Motion is transmitted via a belt and pulley system that connects the stepper motor to the micrometer. A 500 g capacity load cell (DigiKey) is used for force sensing, and 3D-printed fixtures are used to securely mount the specimens. A 2D digital image correlation (DIC) technique is used to analyze the deformation. The specimens are speckled with spray dye to create a pattern to track local deformations. A high-resolution CCD camera (Pike F505B, Allied Vision Technologies) captures images for this analysis. The results of the tensile test, shown in Figure 3.5, indicate that the material exhibits a slightly nonlinear behavior with a small hysteresis during the loading and unloading cycles.

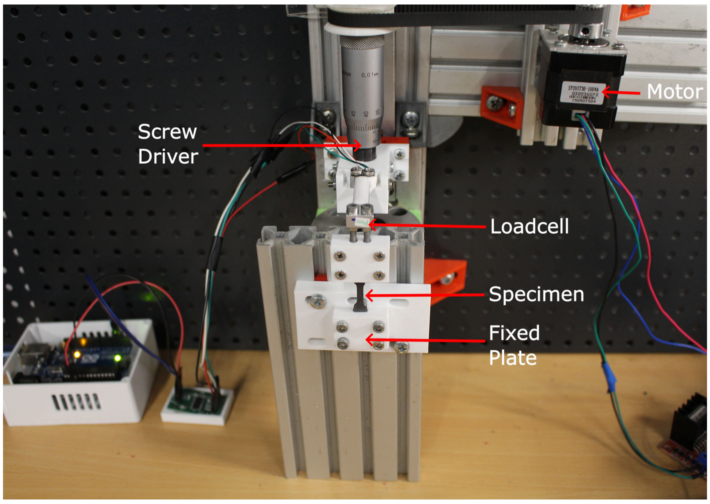

Figure 3.4. Tensile test setup. The screwdriver moves the free end of the specimen upward. Tensile force and strain are recorded simultaneously.

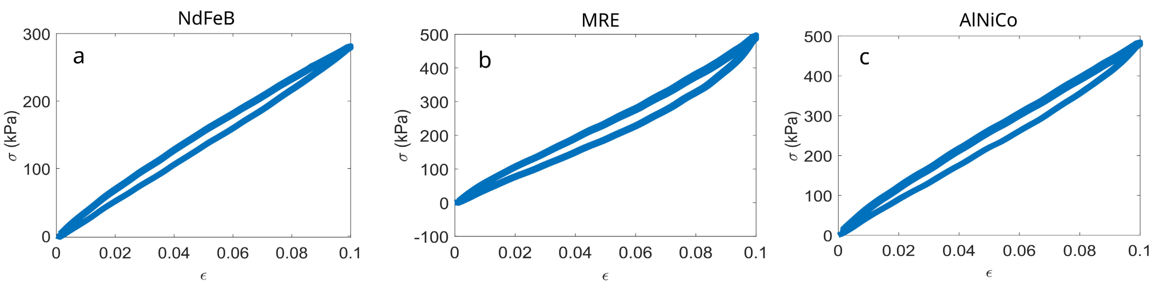

Figure 3.5. The mean stress-strain curves of the soft magnets and the MRE used to manufacture the capsule. The figure shows the response of three different specimens: (a) the NdFeB magnet, (b) the MRE, and (c) the AlNiCo magnet. In the graphs, σ represents stress, and ϵ represents strain.

4. CONCLUSION

In this work it is introduced a reprogrammable magnet which uses a novel concept for reprogramming strategy that goes beyond the current state of the art by eliminating the heat requirement and enabling reprogramming under only a magnetic field. The introduced srPM is a soft counterpart to the classical electro-permanent magnet that is controlled by a magnetic field. Unlike EPM, srPM is operated without a coil on-board allowing for remote functionality.

An srPM can be controlled by a single magnetic pulse allowing switching on and off. The magnetic pulse provides low energy consumption. However, despite the low energy requirement, the magnetic pulse is of high magnitude, requiring significant power. Powering the electromagnets directly from a power supply would require a high-capacity power source, which is typically bulky and expensive. Alternatively, It is used a more efficient and cost-effective solution that is based on a capacitor generating a pulse to provide the required power. Alignment of the magnetic pulse in the srPM is critical for effective operation, which can be challenging. This alignment problem can be overcome by increasing the amplitude of the pulse to ensure reliable state transitions. A magnetic force to hold it in the place can be applied.

The developed srPM measures 6 mm in length and 4 mm in diameter. In the ON state, the srPM exerts a force of 19 mN. In the OFF state, the force decreases to 7 mN. VSM measurements, SEM analysis, tensile tests are performed. Another important outcome of this study is the demonstration of mechanical rotation of magnet powder particles embedded in the elastomer matrix. The rotation of these particles depends on both the shape of the particles and the properties of the elastomer matrix. If these factors can be tuned so that rotation occurs only after a certain threshold. Depending on the selection of the shape and the matrix materials the rotation could be used for magnetic re-programming of soft magnetic robots. Either the rotation can be eliminated and the magnetic properties can directly relate to the application promises.

Another thing to discuss is that the properties of the srPM can be enhanced by applying uni-axial magnetic field during curing. It may result in a higher magnetic field strength enlarging our working space. One thing to discuss is what happens if magnetic field to switch AlNiCo is not enough. Magnetic field strength at the coercivity level will demagnetize AlNiCo, higher magnetic fields will contribute to switching operation, a saturating magnetic field is desired for AlNiCo.

4.1. Contributions and Originality

The state of the art srPM can be switched by a magnetic pulse requiring low energy. The remote reprogramming by magnetic pulses eliminated the tethers making the contribution to the reprogramming strategies. The work of magnetic pulse eliminated the continuous power supply requirement for operation. The contributions can be summarized as (i) remote (in-situ) re-programming via magnetic pulses and (ii) low energy requirement.

This work has contributed to the article papers "A Soft Reprogrammable Permanent Magnet for Magnetic Soft Robots" and "A Magnetically-Actuated Two-Piece Soft Capsule". Two extended abstracts at ICRA@40 and Robosoft 2025 are presented. The srPM concept can be evolved in a robotic application where a moving part on the robot is controlled by an srPM. For example, two robotic applications, one drug delivery capsule and one grasper, are developed using srPM. Other possible applications could be origami robots.

4.2. Outlook and Future Work

The srPM and the method of reprogramming holds promise for future medical applications such as targeted drug delivery and minimally invasive surgery and miniature robots. The design allows for easy scaling and adaptation to meet specific needs as well as modified designs. The fabrication method makes it cost effective and accessible for a wide range of researches. It also holds minimum energy requirement. The application of of magnetic pulses eliminate the necessity of continuous power supply. The achievement of a soft reprogrammable magnet enhances their safety in the event of an accident. The design can be improved by adjusting the geometry allowing for robot applications including locomotion, cargo delivery, meta-materials, origami. It is suitable for on-board use in magnetic soft robots either to modify the magnetic properties of such robots or to actuate certain functionalities. By enabling remote state change, the srPM allows soft magnetic robots to perform specific tasks without physical tethering, complementing their untethered steering capability.

REFERENCES

1. Rus, D. and M. T. Tolley, "Design, Fabrication and Control of Soft Robots", *Nature*, Vol. 521, No. 7553, pp. 467–475, 2015.

2. Yim, S. and M. Sitti, "Design and Rolling Locomotion of a Magnetically Actuated Soft Capsule Endoscope", *IEEE Transactions on Robotics*, Vol. 28, pp. 183–194, 2012.

3. Yim, S., E. Gultepe, D. H. Gracias and M. Sitti, "Biopsy Using a Magnetic Capsule Endoscope Carrying, Releasing, and Retrieving Untethered Microgrippers", *IEEE Transactions on Biomedical Engineering*, Vol. 61, No. 2, pp. 513–521, 2014.

4. Chung, H.-J., A. M. Parsons and L. Zheng, "Magnetically Controlled Soft Robotics Utilizing Elastomers and Gels in Actuation: a Review", *Advanced Intelligent Systems*, Vol. 3, No. 3, p. 2000186, 2021.

5. Wu, S., W. Hu, Q. Ze, M. Sitti and R. Zhao, "Multifunctional Magnetic Soft Composites: a Review", *Multifunctional Materials*, Vol. 3, No. 4, p. 042003, 2020.

6. Mao, Y., K. Yu, M. S. Isakov, J. Wu, M. L. Dunn and H. Jerry Qi, "Sequential Self-Folding Structures by 3D Printed Digital Shape Memory Polymers", *Scientific Reports*, Vol. 5, No. 1, p. 13616, 2015.

7. Kotikian, A., R. L. Truby, J. W. Boley, T. J. White and J. A. Lewis, "3D Printing of Liquid Crystal Elastomeric Actuators with Spatially Programed Nematic Order", *Advanced Materials*, Vol. 30, No. 10, p. 1706164, 2018.

8. Li, T., G. Li, Y. Liang, T. Cheng, J. Dai, X. Yang, B. Liu, Z. Zeng, Z. Huang, Y. Luo, T. Xie and W. Yang, "Fast-moving Soft Electronic Fish", *Science Advances*, Vol. 3, No. 4, p. e1602045, 2017.

9. Iamsaard, S., S. J. Aßhoff, B. Matt, T. Kudernac, J. J. L. M. Cornelissen, S. P. Fletcher and N. Katsonis, "Conversion of Light Into Macroscopic Helical Motion", *Nature Chemistry*, Vol. 6, No. 3, pp. 229–235, 2014.

10. Li, M., X. Wang, B. Dong and M. Sitti, "In-air Fast Response and High Speed Jumping and Rolling of a Light-driven Hydrogel Actuator", *Nature Communications*, Vol. 11, No. 1, p. 3988, 2020.

11. Ranzani, T., G. Gerboni, M. Cianchetti and A. Menciassi, "A Bioinspired Soft Manipulator for Minimally Invasive Surgery", *Bioinspiration & Biomimetics*, Vol. 10, No. 3, p. 035008, 2015.

12. Maeda, S., Y. Hara, R. Yoshida and S. H. and, "Self-Oscillating Gel Actuator for Chemical Robotics", *Advanced Robotics*, Vol. 22, No. 12, pp. 1329–1342, 2008.

13. Hao, Y., S. Zhang, B. Fang, F. Sun, H. Liu and H. Li, "A Review of Smart Materials for the Boost of Soft Actuators, Soft Sensors, and Robotics Applications", *Chinese Journal of Mechanical Engineering*, Vol. 35, No. 1, p. 37, 2022.

14. Zare, M., M. P. Prabhakaran, N. Parvin and S. Ramakrishna, "Thermally-induced Two-way Shape Memory Polymers: Mechanisms, Structures, and Applications", *Chemical Engineering Journal*, Vol. 374, pp. 706–720, 2019.

15. Lum, G. Z., Z. Ye, X. Dong, H. Marvi, O. Erin, W. Hu and M. Sitti, "Shape-programmable Magnetic Soft Matter", *Proceedings of the National Academy of Sciences*, Vol. 113, No. 41, pp. E6007–E6015, 2016.

16. Zhao, R., H. Dai and H. Yao, "Liquid-Metal Magnetic Soft Robot with Reprogrammable Magnetization and Stiffness", *IEEE Robotics and Automation Letters*, Vol. 7, No. 2, pp. 4535–4541, 2022.

17. Wang, H., Z. Zhu, H. Jin, R. Wei, L. Bi and W. Zhang, "Magnetic Soft Robots: Design, Actuation, and Function", *Journal of Alloys and Compounds*, Vol. 922, p.

166219, 2022.

18. Zhou, H., C. C. Mayorga-Martinez, S. Pané, L. Zhang and M. Pumera, "Magnetically Driven Micro and Nanorobots", *Chemical Reviews*, Vol. 121, No. 8, pp. 4999–5041, 2021.

19. Gao, Y., F. Wei, Y. Chao and L. Yao, "Bioinspired Soft Microrobots Actuated by Magnetic Field", *Biomedical Microdevices*, Vol. 23, No. 4, p. 52, 2021.

20. Rikken, R. S. M., R. J. M. Nolte, J. C. Maan, J. C. M. van Hest, D. A. Wilson and P. C. M. Christianen, "Manipulation of micro- and nanostructure motion with magnetic fields", *Soft Matter*, Vol. 10, pp. 1295–1308, 2014.

21. Kim, Y. and X. Zhao, "Magnetic Soft Materials and Robots", *Chemical Reviews*, Vol. 122, No. 5, pp. 5317–5364, 2022, pMID: 35104403.

22. Knaian, A. N., *Electropermanent Magnetic Connectors and Actuators: Devices and Their Application in Programmable Matter*, Ph.D. Thesis, Massachusetts Institute of Technology, 2010.

23. Velez, C., L. P. Tatum, B. S. Herstein, C. P. Becker and D. P. Arnold, "Batch-fabrication and Characterization of Miniaturized Axisymmetric Electropermanent Magnets", *Journal of Physics: Conference Series*, Vol. 1052, No. 1, p. 012045, 2018.

24. Leps, T., P. E. Glick, D. R. III, A. Parness, M. T. Tolley and C. Hartzell, "A Low-power, Jamming, Magnetorheological Valve Using Electropermanent Magnets Suitable for Distributed Control in Soft Robots", *Smart Materials and Structures*, Vol. 29, No. 10, p. 105025, 2020.

25. Gholizadeh, A., S. Abbaslou, P. Xie, A. Knaian and M. Javanmard, "Electronically Actuated Microfluidic Valves with Zero Static-power Consumption Using Electropermanent Magnets", *Sensors and Actuators A: Physical*, Vol. 296, pp.

316–323, 2019.

26. Marchese, A. D., C. D. Onal and D. Rus, *Towards a Self-contained Soft Robotic Fish: On-Board Pressure Generation and Embedded Electro-permanent Magnet Valves*, pp. 41–54, Springer International Publishing, Heidelberg, 2013.

27. Padovani, J. I., S. S. Jeffrey and R. T. Howe, “Electropermanent Magnet Actuation for Droplet Ferromicrofluidics”, *Technology*, Vol. 04, No. 02, pp. 110–119, 2016.

28. McDonald, K. J., L. Kinnicutt, A. M. Moran and T. Ranzani, “Modulation of Magnetorheological Fluid Flow in Soft Robots Using Electropermanent Magnets”, *IEEE Robotics and Automation Letters*, Vol. 7, No. 2, pp. 3914–3921, 2022.

29. Johnson, W. R., S. J. Woodman and R. Kramer-Bottiglio, “An Electromagnetic Soft Robot that Carries its Own Magnet”, *IEEE 5th International Conference on Soft Robotics (RoboSoft)*, pp. 761–766, Edinburgh, UK, 2022.

30. Bolanakis, G. and E. Papadopoulos, “Introducing Mag-Nets: Rapidly Bending Electromagnetic Actuators for Self-Contained Soft Robots”, *IEEE Robotics and Automation Letters*, Vol. PP, pp. 1–8, 2024.

31. Moran, A. M., V. T. Vo, K. J. McDonald, P. Sultania, E. Langenbrunner, J. H. V. Chong, A. Naik, L. Kinnicutt, J. Li and T. Ranzani, “An Electropermanent Magnet Valve for the Onboard Control of Multi-degree of Freedom Pneumatic Soft Robots”, *Communications Engineering*, Vol. 3, No. 1, p. 117, 2024.

32. Gaeta, L. T., K. J. McDonald, L. Kinnicutt, M. Le, S. Wilkinson-Flicker, Y. Jiang, T. Atakuru, E. Samur and T. Ranzani, “Magnetically induced stiffening for soft robotics”, *Soft Matter*, Vol. 19, pp. 2623–2636, 2023.

33. Zhang, P., M. Kamezaki, Z. He, H. Sakamoto and S. Sugano, “EPM–MRE: Electro Permanent Magnet–Magnetorheological Elastomer for Soft Actuation System and Its Application to Robotic Grasping”, *IEEE Robotics and Automation Letters*,

Vol. 6, No. 4, pp. 8181–8188, 2021.

34. Shirazee, N. and A. Basak, “Electropermanent Suspension System for Acquiring Large Air-gaps to Suspend Loads”, *IEEE Transactions on Magnetics*, Vol. 31, No. 6, pp. 4193–4195, 1995.

35. Knaian, A. N., K. C. Cheung, M. B. Lobovsky, A. J. Oines, P. Schmidt-Neilsen and N. A. Gershenfeld, “The Milli-Motein: Self-Folding Chain of Programmable Matter with a One Centimeter Module Pitch”, *IEEE/RSJ International Conference on Intelligent Robots and Systems*, pp. 1447–1453, St Paul, USA, 2012.

36. Zhou, C., Y. Yang, J. Wang, Q. Wu, Z. Gu, Y. Zhou, Y. Zhang, Y. Liu, Y. Wang, Y. Zhu and X. Liu, “Ferromagnetic Soft Catheter Robots for Minimally Invasive Bioprinting”, *Nature Communications*, Vol. 12, No. 1, p. 5072, 2021.

37. Roghani, M., D. Romeis, D. Borin and M. Saphiannikova, “Influence of Matrix Stiffness on Microstructure Evolution and Magnetization of Magneto-active Elastomers”, *Soft Matter*, Vol. 21, pp. 1416–1425, 2025.

38. Pagoli, A., F. Chapelle, J.-A. Corrales-Ramon, Y. Mezouar and Y. Lapusta, “Review of Soft Fluidic Actuators: Classification and Materials Modeling Analysis”, *Smart Materials and Structures*, Vol. 31, No. 1, p. 013001, 2021.

39. Lu, X., X. Qiao, H. Watanabe, X. Gong, T. Yang, W. Li, K. Sun, M. Li, K. Yang, H. Xie, Q. Yin, D. Wang and X. Chen, “Mechanical and Structural Investigation of Isotropic and Anisotropic Thermoplastic Magnetorheological Elastomer Composites Based on Poly(styrene-b-ethylene-co-butylene-b-styrene) (SEBS)”, *Rheologica Acta*, Vol. 51, No. 1, pp. 37–50, 2012.

40. An, H.-N., B. Sun, S. J. Picken and E. Mendes, “Long Time Response of Soft Magnetorheological Gels”, *The Journal of Physical Chemistry B*, Vol. 116, No. 15, pp. 4702–4711, 2012.

41. An, H.-N., S. J. Picken and E. Mendes, "Direct observation of particle rearrangement during cyclic stress hardening of magnetorheological gels", *Soft Matter*, Vol. 8, pp. 11995–12001, 2012.

42. Sitti, M., H. Ceylan, W. Hu, J. Giltinan, M. Turan, S. Yim and E. D. Diller, "Biomedical Applications of Untethered Mobile Milli/Microrobots", *Proceedings of the IEEE*, Vol. 103, pp. 205–224, 2015.

43. Lu, H., M. Zhang, Y. Yang, Q. Huang, T. Fukuda, Z. Wang and Y. Shen, "A Bioinspired Multilegged Soft Millirobot That Functions in Both Dry and Wet Conditions", *Nature Communications*, Vol. 9, No. 1, pp. 3944–3945, 2018.

44. Nelson, B. J., I. K. Kaliakatsos and J. J. Abbott, "Microrobots for Minimally Invasive Medicine", *Annual Review of Biomedical Engineering*, Vol. 12, No. 1, pp. 55–85, 2010, pMID: 20415589.

45. Sitti, M., "Voyage of the Microrobots", *Nature*, Vol. 458, No. 7242, pp. 1121–1122, 2009.

46. Song, H., H. Lee, J. Lee, J. K. Choe, S. Lee, J. Y. Yi, S. Park, J.-W. Yoo, M. S. Kwon and J. Kim, "Reprogrammable Ferromagnetic Domains for Reconfigurable Soft Magnetic Actuators", *Nano Letters*, Vol. 20, No. 7, pp. 5185–5192, 2020, pMID: 32491865.

47. Bira, N., P. Dhagat and J. R. Davidson, "A Review of Magnetic Elastomers and Their Role in Soft Robotics", *Frontiers in Robotics and AI*, Vol. 7, 2020.588391.

48. Bowen, L., K. Springsteen, H. Feldstein, M. Frecker, T. W. Simpson and P. von Lockette, "Development and Validation of a Dynamic Model of Magneto-Active Elastomer Actuation of the Origami Waterbomb Base", *Journal of Mechanisms and Robotics*, Vol. 7, No. 1, p. 011010, 2015.

49. Hadzir, M. N. H., M. H. Abu Bakar and I. A. Azid, *Effect of the Magnetic Field on*

Magnetic Particles in Magnetorheological Elastomer Layers, pp. 135–143, Springer International Publishing, Cham, 2019.

50. Coquelle, E. and G. Bossis, “Mullins Effect in Elastomers Filled with Particles Aligned by a Magnetic Field”, *International Journal of Solids and Structures*, Vol. 43, No. 25, pp. 7659–7672, 2006.

51. Dorfmann, A. and R. Ogden, “Magnetoelastic Modelling of Elastomers”, *European Journal of Mechanics - A/Solids*, Vol. 22, No. 4, pp. 497–507, 2003.

52. Bastola, A. K. and M. Hossain, “A Review on Magneto-mechanical Characterizations of Magnetorheological Elastomers”, *Composites Part B: Engineering*, Vol. 200, p. 108348, 2020.

53. Diguet, G., E. Beaugnon and J. Cavaillé, “Shape Effect in the Magnetostriction of Ferromagnetic Composite”, *Journal of Magnetism and Magnetic Materials*, Vol. 322, No. 21, pp. 3337–3341, 2010.

54. Ebrahimi, N., C. Bi, D. J. Cappelleri, G. Ciuti, A. T. Conn, D. Faivre, N. Habibi, A. Hošovský, V. Iacovacci, I. S. M. Khalil, V. Magdanz, S. Misra, C. Pawashe, R. Rashidifar, P. E. D. Soto-Rodriguez, Z. Fekete and A. Jafari, “Magnetic Actuation Methods in Bio/Soft Robotics”, *Advanced Functional Materials*, Vol. 31, No. 11, p. 2005137, 2021.

55. Schmitt, F., O. Piccin, L. Barbé and B. Bayle, “Soft Robots Manufacturing: A Review”, *Front Robot AI*, Vol. 5, p. 84, 2018.

56. Xu, T., J. Yu, X. Yan, H. Choi and L. Zhang, “Magnetic Actuation Based Motion Control for Microrobots: an Overview”, *Micromachines*, Vol. 6, No. 9, pp. 1346–1364, 2015.

57. Ginder, J. M., S. M. Clark, W. F. Schlotter and M. E. Nichols, “Magnetostrictive Phenomena in Magnetorheological Elastomers”, *International Journal of Modern*

Physics B, Vol. 16, No. 17n18, pp. 2412–2418, 2002.

58. Schümann, M. and S. Odenbach, "In-situ Observation of the Particle Microstructure of Magnetorheological Elastomers in Presence of Mechanical Strain and Magnetic Fields", *Journal of Magnetism and Magnetic Materials*, Vol. 441, pp. 88–92, 2017.

59. Martin, J. E., R. A. Anderson, D. Read and G. Gulley, "Magnetostriction of Field-structured Magnetoelastomers", *Phys. Rev. E*, Vol. 74, p. 051507, 2006.

60. Danas, K., S. Kankanala and N. Triantafyllidis, "Experiments and Modeling of Iron-particle-filled Magnetorheological Elastomers", *Journal of the Mechanics and Physics of Solids*, Vol. 60, No. 1, pp. 120–138, 2012.

61. Han, Y., A. Mohla, X. Huang, W. Hong and L. E. Faidley, "Magnetostriction and Field Stiffening of Magneto-Active Elastomers", *International Journal of Applied Mechanics*, Vol. 07, No. 01, p. 1550001, 2015.

62. Guan, X., X. Dong and J. Ou, "Magnetostrictive Effect of Magnetorheological Elastomer", *Journal of Magnetism and Magnetic Materials*, Vol. 320, No. 3, pp. 158–163, 2008.

63. Bednarek, S., "The Giant Magnetostriction in Ferromagnetic Composites Within an Elastomer Matrix", *Applied Physics A*, Vol. 68, No. 1, pp. 63–67, 1999.

64. Han, Y., W. Hong and L. E. Faidley, "Field-stiffening Effect of Magneto-rheological Elastomers", *International Journal of Solids and Structures*, Vol. 50, No. 14, pp. 2281–2288, 2013.

65. Varga, Z., G. Filipcsei and M. Zrínyi, "Magnetic Field Sensitive Functional Elastomers with Tuneable Elastic Modulus", *Polymer*, Vol. 47, No. 1, pp. 227–233, 2006.

66. Schmauch, M. M., S. R. Mishra, E. E. Evans, O. D. Velev and J. B. Tracy, "Chained Iron Microparticles for Directionally Controlled Actuation of Soft Robots", *ACS Applied Materials & Interfaces*, Vol. 9, No. 13, pp. 11895–11901, 2017.

67. Mishra, S. R., M. D. Dickey, O. D. Velev and J. B. Tracy, "Selective and Directional Actuation of Elastomer Films Using Chained Magnetic Nanoparticles", *Nanoscale*, Vol. 8, pp. 1309–1313, 2016.

68. Kim, J., S. E. Chung, S.-E. Choi, H. Lee, J. Kim and S. Kwon, "Programming Magnetic Anisotropy in Polymeric Microactuators", *Nature Materials*, Vol. 10, No. 10, pp. 747–752, 2011.

69. Roeder, L., P. Bender, A. Tschöpe, R. Birringer and A. M. Schmidt, "Shear Modulus Determination in Model Hydrogels by Means of Elongated Magnetic Nanoprobes", *Journal of Polymer Science Part B: Polymer Physics*, Vol. 50, No. 24, pp. 1772–1781, 2012.

70. Lisjak, D. and A. Mertelj, "Anisotropic Magnetic Nanoparticles: a Review of Their Properties, Syntheses and Potential Applications", *Progress in Materials Science*, Vol. 95, pp. 286–328, 2018.

71. Seifert, J., S. Roitsch and A. M. Schmidt, "Covalent Hybrid Elastomers Based on Anisotropic Magnetic Nanoparticles and Elastic Polymers", *ACS Applied Polymer Materials*, Vol. 3, No. 3, pp. 1324–1337, 2021.

72. Hu, W., G. Z. Lum, M. Mastrangeli and M. Sitti, "Small-scale Soft-bodied Robot with Multimodal Locomotion", *Nature*, Vol. 554, No. 7690, pp. 81–85, 2018.

73. Kim, Y., G. A. Parada, S. Liu and X. Zhao, "Ferromagnetic Soft Continuum Robots", *Science Robotics*, Vol. 4, No. 33, p. eaax7329, 2019.

74. Xu, T., J. Zhang, M. Salehizadeh, O. Onaizah and E. Diller, "Millimeter-scale Flexible Robots with Programmable Three-dimensional Magnetization and Motions",

Science Robotics, Vol. 4, p. eaav4494, 2019.

75. Kim, Y., H. Yuk, R. Zhao, S. A. Chester and X. Zhao, "Printing Ferromagnetic Domains for Untethered Fast-transforming Soft Materials", *Nature*, Vol. 558, pp. 274–279, 2018.

76. Huang, H.-W., M. S. Sakar, A. J. Petruska, S. Pané and B. J. Nelson, "Soft Micromachines with Programmable Motility and Morphology", *Nature Communications*, Vol. 7, p. 12263, 2016.

77. Ze, Q., X. Kuang, S. Wu, J. Wong, S. M. Montgomery, R. Zhang, J. M. Kovitz, F. Yang, H. J. Qi and R. Zhao, "Magnetic Shape Memory Polymers with Integrated Multifunctional Shape Manipulation", *Advanced Materials*, Vol. 32, No. 4, p. 1906657, 2020.

78. Cui, J., T.-Y. Huang, Z. Luo, P. Testa, H. Gu, X.-Z. Chen, B. J. Nelson and L. J. Heyderman, "Nanomagnetic Encoding of Shape-morphing Micromachines", *Nature*, Vol. 575, No. 7781, pp. 164–168, 2019.

79. Alapan, Y., A. C. Karacakol, S. N. Guzelhan, I. Isik and M. Sitti, "Reprogrammable Shape Morphing of Magnetic Soft Machines", *Science Advances*, Vol. 6, No. 38, p. 6414, 2020.

80. Gong, Y., Y. Li, Y. Zhao, P. Li, L. Yi, P. Liu, X. Chen, J. Zhan, Y. Zheng, H. Li and F. Liu, "Magnetic Material Gradient-distributed Soft Actuators Via Magnetic Field-assisted Laser Direct Writing", *Chemical Engineering Journal*, Vol. 515, p. 163937, 2025.

81. Wu, Y., S. Zhang, Y. Yang, Z. Li, Y. Wei and Y. Ji, "Locally Controllable Magnetic Soft Actuators with Reprogrammable Contraction-derived Motions", *Science Advances*, Vol. 8, No. 25, p. eabo6021, 2022.

82. Yang, B., R. Baines, D. Shah, S. Patiballa, E. Thomas, M. Venkadesan and

R. Kramer-Bottiglio, “Reprogrammable Soft Actuation and Shape-shifting Via Tensile Jamming”, *Science Advances*, Vol. 7, No. 40, p. eabh2073, 2021.

83. Deng, H., K. Sattari, Y. Xie, P. Liao, Z. Yan and J. Lin, “Laser Reprogramming Magnetic Anisotropy in Soft Composites for Reconfigurable 3D Shaping”, *Nature Communications*, Vol. 11, No. 1, p. 6325, 2020.

84. Cao, L., D. Yu, Z. Xia, H. Wan, C. Liu, T. Yin and Z. He, “Ferromagnetic Liquid Metal Putty-Like Material with Transformed Shape and Reconfigurable Polarity”, *Advanced Materials*, Vol. 32, No. 17, p. 2000827, 2020.

85. Kuang, X., S. Wu, Q. Ze, L. Yue, Y. Jin, S. M. Montgomery, F. Yang, H. J. Qi and R. Zhao, “Magnetic Dynamic Polymers for Modular Assembling and Reconfigurable Morphing Architectures”, *Advanced Materials*, Vol. 33, No. 30, p. 2102113, 2021.

86. Dong, G., Q. He and S. Cai, “Magnetic Vitrimer-Based Soft Robotics”, *Soft Matter*, Vol. 18, pp. 7604–7611, 2022.

87. Li, W., H. Chen, Z. Yi, F. Fang, X. Guo, Z. Wu, Q. Gao, L. Shao, J. Xu, G. Meng and W. Zhang, “Self-vectoring Electromagnetic Soft Robots with High Operational Dimensionality”, *Nature Communications*, Vol. 14, No. 1, p. 182, 2023.

88. Liu, Y., J. Huang, C. Liu, Z. Song, J. Wu, Q. Zhao, Y. Li, F. Dong, L. Wang and H. Xu, “Soft Millirobot Capable of Switching Motion Modes on the Fly for Targeted Drug Delivery in the Oviduct”, *ACS Nano*, Vol. 18, No. 12, pp. 8694–8705, 2024, pMID: 38466230.

89. Johnson, W. R. and R. Kramer-Bottiglio, “Compliant Electropermanent Magnets”, *IEEE 7th International Conference on Soft Robotics (RoboSoft)*, pp. 347–352, San Diego, CA, USA, 2024.

90. Vaganov, M. V., D. Y. Borin, S. Odenbach and Y. L. Raikher, “Mesomagnetome-

chanics of Hybrid Elastomer Composites: Magnetization of Elastically Trapped Particles", *Journal of Magnetism and Magnetic Materials*, Vol. 499, p. 166249, 2020.

91. Stepanov, G. V., D. Y. Borin, A. V. Bakhtiiarov and P. A. Storozhenko, "Magnetic Properties of Hybrid Elastomers with Magnetically Hard Fillers: Rotation of Particles", *Smart Materials and Structures*, Vol. 26, p. 035060, 2017.

92. Sodomka, O. and F. Mach, "Electrically Switchable Magnetic Elastomer", *AIP Advances*, Vol. 15, No. 3, p. 035117, 2025.

93. Sun, Y., B. Sun, X. Cui, W. Li, Y. Zhang, L. He, S. Nong, Z. Zhu, J. Wu, D. Li, X. Li, S. Zhang, X. Li and M. Li, "Addressable and Perceptible Dynamic Reprogram of Ferromagnetic Soft Machines", *Nature Communications*, Vol. 16, No. 1, p. 2267, 2025.

94. Magnequench, "MQP-S-11-9-20001", `https://mqitechnology.com/product/mqp-s-11-9-20001/`, 2017, accessed on Jun. 3, 2017.

95. Sabciyan, A. I., *Ozel Miknatislayici Tasarimi*, Master's Thesis, Istanbul Teknik Universitesi, 2007.

96. Vaganov, M., D. Borin, S. Odenbach and Y. Raikher, "Effect of Local Elasticity of the Matrix on Magnetization Loops of Hybrid Magnetic Elastomers", *Journal of Magnetism and Magnetic Materials*, Vol. 459, pp. 92–97, 2018.

APPENDIX A: DATASHEETS

For further information see [94].

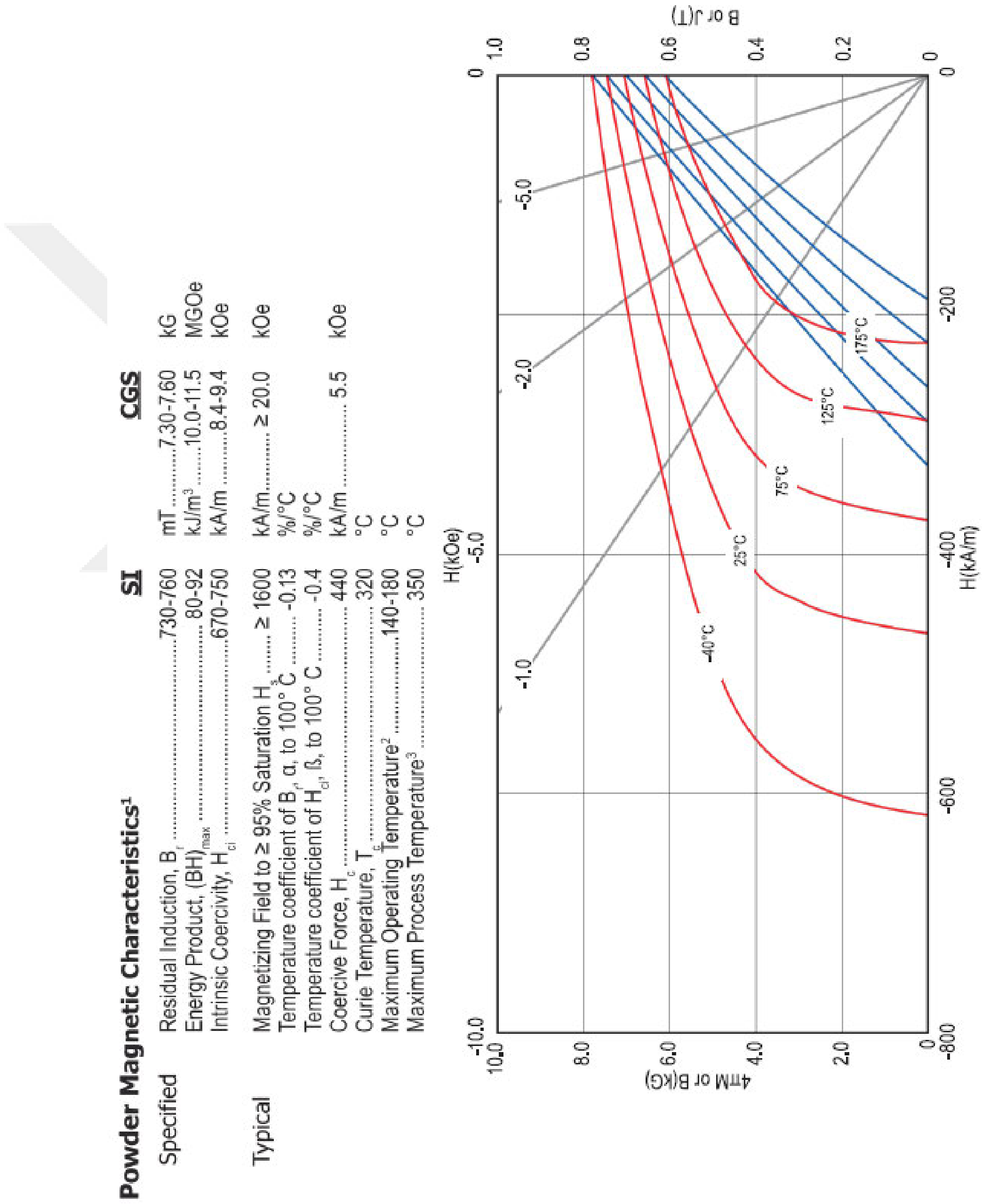

Figure A.1. Magnetic properties of mqp-s-11-9-20001, NdFeB powder.